The 22 December 2018 Mount Anak Krakatau Volcanogenic Tsunami on Sunda Strait Coasts, Indonesia: tsunami and damage characteristics

Syamsidik[1,2], Benazir[1,2], Mumtaz Luthfi[1], Anawat Suppasri[3], and Louise K. Comfort[4]

[1] Tsunami and Disaster Mitigation Research Centre (TDMRC), Universitas Syiah Kuala, Jl. Prof. Dr. Ibrahim Hasan, Gampong Pie, Banda Aceh, 23233 Indonesia.

[2] Civil Engineering Department, Faculty of Engineering, Universitas Syiah Kuala, Jl. Syeh Abdurrauf No. 7, Banda Aceh, 23111 Indonesia.

[3] International Research Institute of Disaster Science (IRIDeS), Tohoku University, Aramaki Aza-Aoba 468-1, Aoba-ku, Sendai 980-0845, Japan, email: suppasri@irides.tohoku.ac.jp

[4] Graduate School of Public International Affairs, University of Pittsburgh, Pittsburgh, United States of America, email: lkc@pitt.edu

Correspondence to: Syamsidik (syamsidik@tdmrc.org, syamsidik@unsyiah.ac.id)

ABSTRACT

On 22 December 2018, a tsunami was generated from the Mount Anak Krakatau area that was caused by volcanic flank failures. The tsunami had severe impacts on the western coast of Banten and the southern coasts of Lampung in Indonesia. A series of surveys to measure the impacts of the tsunami was started three days after the tsunami and lasted ten days. Immediate investigations allowed the collection of relatively authentic images of the tsunami impacts before the clearing process started. This article investigates the impacts of the 2018 Sunda Strait tsunami on the affected areas and presents an analysis of the impacts of pure hydrodynamic tsunami forces on buildings. Impacts of the tsunami were expected to exhibit different characteristics than those found following the 2004 Indian Ocean tsunami in Aceh. Data was collected from 117 flow depths along the Banten and Lampung coasts. Furthermore, 98 buildings or houses were assessed for damage. Results of this study revealed that the flow depths were higher in Banten than in Lampung. Directions of the tsunami arrays created by the complex bathymetry around the strait caused these differences. Tsunami-induced damage to buildings was mostly the result of impact forces and drag forces. Damping forces could not be associated with the damages. The tsunami warning system in Indonesia should be extended to anticipate non-seismic tsunamis, such as landslides and volcanic processes driven by tsunamis. Lack of a tsunami warning during the first few minutes after the generation of the first wave led to a significant number of human casualties at both of the affected areas.

1 Introduction

In 2018, there were two important tsunami disasters that drew the attention of disaster researchers, namely the 28 September 2018 Palu tsunami, and the 22 December 2018 Sunda Strait Tsunami. The latter was generated by the Mount Anak Krakatau volcanic eruption. An official number of human casualties reported was 437 dead, 31,942 injured, and 10 still missing as of completion of this report

(BNPB, 2019). Local area communities received no warning of the 22 December 2018 tsunami that was generated by the Anak Krakatau. This was one reason for the large number of human casualties on both sides of the affected area. What made this tsunami of particular interest was the rare process that led to its generation, and the fact that it occurred at night, hindering any direct visual anticipation and interaction by area communities.

In some cases, people living around the volcano are not well prepared to face a potential tsunami that can be generated by eruptions. This was the case was for those communities around the Thyrrenian coast of Italy (Teresita et al., 2019). Sustained public engagement is necessary, as in the Mount Zao case in Japan (Donovan et al., 2018). As the record of volcanogenic tsunamis is long, proper mitigation of non-tectonic tsunamis could be difficult in practice.

Volcanic eruption-induced tsunamis have been recorded at several locations, including one that occurred in 1883 due to the Mount Krakatau Eruption. This tsunami caused between 30,000 and 70,000 deaths and affected not only the surrounding coasts along the Sunda Strait, but also Madagascar on the western edge of the Indian Ocean basin, located about 3,000 km from the Mount Krakatau Complex (Choi et al., 2003). The highest wave reported due to the eruption was 40 m (Spicak et al., 2008). The 1883 eruption deformed the main dome of the Krakatau into four parts, i.e. Rakata Island, Sertung Island, Lang Island and Anak Krakatau. The crater of Krakatau was flattened under water due to the 1883 eruption; it emerged to the surface in 1930 and was named Mount Anak Krakatau, which literally means 'the child of Krakatau (Bani et al., 2015; Zen, 1970).' Mount Anak Krakatau is considered among the most active volcanos in the world. Before the 2018 eruption, it erupted 40 times over the past 85 years (GVP, 2019). Nonetheless, only the 2018 eruption caused a tsunami wave that affected the southern coast of Sumatra (Lampung Province) and the western coast of Java Island (Banten Province). In 2012, Giachetti et al. identified an active zone at the southwestern flank of Mount Anak Krakatau that expanded from time to time. They also revealed that the southwestern flank failure could generate a-45 m wave toward the small islands surrounding the volcano complex that could reach the Banten area with 1.5 m wave heights within 35–45 minutes after the collapse (Giachetti et al., 2012). The growth of Mount Anak Krakatau was observed toward the southwest based on a survey in 1994 (Deblus et al., 1995). This made the slope of the southwestern flank significantly steep, inclined at about 0.9 as of 1995. The southwestern flank failure could also be associated with the tsunami that occurred in 1981 (Sigurdsson et al., 1991) despite no record of human casualties. Despite the long record of Anak Krakatau events, the 2018 tsunami in Sunda Strait still caused a significant number of human casualties, and impacts on the coastal settlement area were severe. The 22 December 2018 Mount Anak Krakatau tsunami was caused by a small volume of southwestern flank failure (<0.25 km^3) of the volcano (Williams et al., 2019). Prior to this tsunami, the Government of Indonesia released a status of the activities of Mount Anak Krakatau that has been active since June 2018 (PVMBG, 2018).

This study investigates the impacts of volcanogenic tsunamis, generated by Mount Anak Krakatau, on Lampung and Banten, located around Sunda Strait, Indonesia. A series of measurements were performed at the affected area from 24 December 2018 until 3 January 2019. Data collected in this research were

compiled in a database that is stored at the Mendeley database (Syamsidik et al., 2019b). Some locations with measured flow depths, damaged buildings and tsunami boulders can be referenced by the database. In this article, reported impacts of the tsunami on buildings provide novel findings where field tsunami impact data has mostly been based on tectonic tsunamis. Here we present results of an analysis of the

5   damage to buildings due purely to tsunami hydrodynamic forces. Notwithstanding the presented findings, we acknowledge some limitations of the study as elucidated in Section 6, Discussions and Limitations. This article is expected to contribute to tsunami engineering studies, and to a better understanding of tsunami mitigation efforts, especially on analysis of damage to buildings due to tsunamis.

10   **2 Survey Area**

The tsunami-affected area was largely reported to be from the southern coasts of Lampung and western coasts of Banten. In this study, we investigated five areas as shown in **Fig. 1**. Two areas were Pandeglang district and Serang District of the western coasts of Banten. The other three areas were South Lampung

15   and Tanggamus districts of Lampung Province. Serang District has a total population of about 1.56 million as of 2017, while Pandeglang has a total population about 1.21 million as of 2017. Serang is famous for its industrial areas, where a large steel company is located at its coast. Pandeglang is known for tourism, where a number of hotels and resorts, located along its coast, are heavily occupied during the long holiday season. Some areas in Pandeglang were difficult to assess using land transportation due

20   to road damage, and some routes are still not constructed. This made it difficult to investigate the most southern part of Pandeglang. Along Banten, we investigated about 112 km of its coastlines.

In Lampung area, about 57 km of coastline were investigated, covering the two districts at the southern part of the province. South Lampung district has a population of about 980 thousand people, most of whom reside at the coastal area. Kalianda is the capital city of the district, which was also affected by

25   the 2018 Sunda Strait Tsunami. Another area in the district that was affected by the tsunami is Rajabasa. People in the two areas are mainly farmers and fishermen. A large ferry port accommodating a number of ferry lanes servicing Banten and Lampung is located in this district. Fortunately, there was no major impact on the port. The other district in Lampung investigated in this study is Tanggamus. Here, only one victim reportedly died from the tsunami. We investigated a small bay where human casualties were

30   reported in this district.

Fig. 1. Surveyed area following the 22 December 2018 Mount Anak Krakatau volcanogenic tsunami.
35   Five areas of the survey are marked in blue-rectangular. Tidal-gauge stations are marked in green triangles. Bathymetry data was adopted from Topex (2019).

3 Methods

3.1 Survey method

A series of surveys was conducted at the five affected areas as explained in the previous section from 24
December 2018 until 3 January 2019. The ten-day survey was initiated to measure the impacts of the
tsunami on Banten area. In this area, the team spent six days measuring tsunami flow depths, tsunami
boulders, and damage to housing or buildings in the affected area. Another four days of the survey were
spent in Lampung area measuring the same data. Measurement of flow depths was done using a levelling
staff and water pass to measure water marks, broken twigs, or stranded tsunami debris. A handheld GPS
was used to locate the coordinates of the measured flow depths. The GPS was also used to measure limit
of tsunami inundation. A similar method was used to measure impacts of the 29 September 2009
American Samoa tsunami and the 1946 Aleutian tsunami, the 2004 Indian Ocean tsunami in Banda Aceh
(Borrero et al., 2006), and the 2018 Palu tsunami (Syamsidik et al., 2019a). A drone was also utilised in
this survey to capture images from the tsunami-affected area. In total, we managed to measure 117 flow
depths from both sides of the affected area. All data was stored in the Mendeley dataset (Syamsidik et
al., 2019b). The survey was not performed at offshore islands around Mount Anak Krakatau, as the area
was restricted by the Government for any activity due to the threat of volcanic activity and the tsunamis.

The tsunami arrival at the coastal area was analysed based on water elevations measured at four tidal-
gauge stations. The locations of the tidal-gauge stations can be seen in **Fig. 1**. To separate the tsunami
wave data from the long-frequency data influenced by astronomical components, a low pass filter was
applied. Threshold frequency for the filtering was 0.0805 cycle per day (cpd) as suggested by Emery and
Thomson (2001). Arrival times were interpreted based on the first peak of the wave recorded at the tidal-
gauge stations. To confirm the conditions around the arrival times of the tsunami, we also performed a
number of interviews in the local community. Three main questions were asked, i.e. indications or some
sign before the tsunami arrived, the number of waves, and the evacuation process. Ten persons were
asked at the Banten coasts and five in Lampung. Since the number of interviewees was limited, results
of the interviews were meant to confirm the conditions before the tsunami arrival qualitatively.

3.2 Velocity Inferred Tsunami Boulders

Velocity data was inferred from tsunami boulder transportation. Types of boulders were classified based
on size and material composition. During the survey, they were dominated by two kinds of boulder
materials, namely coral and ruble mound material from revetment structures. A description of the
analytical solutions for inferring tsunami boulder transportation was given by Noormets et al. (2004).
Tsunami boulders were measured for their dimensions, original locations (based on interviews and
materials), and distance of transport. Tsunami boulder transportation velocities were inferred using eq
(1), as suggested by Paris et al. (2010):

$$u_{min} = \sqrt{\frac{2\mu m g}{C_d A_n \rho_w}} \, , \qquad\qquad (1)$$

where u_{min} is minimum estimated velocity (m/s), µ is friction coefficient, which is 0.7 as suggested by Noormets et al. (2004), g is gravitational acceleration (m/s^2), C_d is drag coefficient, which was considered as 1.95, A_n is the areal of the boulder perpendicular to the tsunami flow direction, and ρ_w is water density (1027 kg/m^3).

5 Distance travelled by the tsunami boulder depended on tsunami velocity, size of the boulder, and boulder material. The range of seawall material transported as a tsunami boulder was 3–4 m/s for sliding or rolling movement, and 11–12 m/s if the boulder moved as a saltation mode (Nandasena et al., 2011; Paris et al., 2009).

10 **3.3 Building Damage Observations**

Assessment of building damage was performed on 98 buildings, most of them houses. Among the assessed buildings, 73 were confined masonry-brick infill houses. This type of house used smooth bar as structural components and masonry fill for walls. The walls were strengthened by tie-columns and tie-beams at the tops. Most of walls had a thickness of 15 cm. The bricks were bound by about 2–3 cm

15 mortars. Plain bars were used to connect the walls with windows and door elements. This type of house predominated in Banten and Lampung areas. A similar type of house was found to be the majority of houses in the 2004 Indian Ocean tsunami-affected area in Aceh. Around 70% of the houses in Aceh were confined-masonry-brick infill houses (EERI, 2006; Boen, 2005; Brzev, 2007). This allowed for comparison between cases in the 2004 Indian Ocean and 2018 Mount Anak Krakatau tsunamis.

The types of the damage were classified into five damage states (DS) as suggested by Suppasri et al. (2014) and Macabuag et al. (2016). The list of DS classifications can be seen in **Table 1**. To exclude houses altered due to clearing processes, the assessment was limited to the confined masonry-brick infill buildings (CM) and wooden houses. Types of houses in the Banten and Lampung affected areas were

25 relatively similar. Most of the buildings located near the coastal areas functioned as residences or villas/cottages.

Data collected was analysed using fragility functions to produce cumulative probabilities of damage caused by the tsunami. Equation (2) was used to calculate the fragility functions:

30 $$P(x) = \phi \left[\frac{x-\mu}{\sigma} \right], \qquad\qquad (2)$$

where P is the cumulative probability of damage, ϕ is the standardised normal distribution function, x is the hydrodynamic feature analysed for damage (in this case, flow depth), and μ and σ are mean and standard deviations of x, respectively.

35 The fragility function was developed to estimate the future impacts of a tsunami. In previous cases, the function was developed based on tectonic tsunamis (Koshimura et al., 2009; Suppasri et al., 2015). In this study, as there was no earthquake preceding the tsunami, analysis of the damage was based purely on tsunami wave propagation.

Table 1. Damage states of buildings due to tsunamis as suggested by Suppasri et al. (2011) and Macabuag et al. (2016).

4   Results

4.1 Tsunami Arrival Times

Tsunami arrivals were determined based on water elevations monitored at four tidal-gauge stations located around the Sunda Strait. The stations were Marina Jambu, Ciwandan, Panjang and Kota Agung. The tidal-gauge stations are operated by Indonesia Geospatial Information Agency (BIG). Each of the stations recorded one-minute interval water levels and are available online. **Fig. 2** shows the filtered tidal data from all four stations. The first detected tsunami wave arrival was recorded at Marina Jambu Station at 14.30 UTC (at 09.30 PM local time). The time of generation of the tsunami from the source was not clear since no tidal station was located around the volcano. Ten minutes later (14.43 UTC), the tsunami wave was recorded at Ciwandan station, near Cilegon, Banten. The first tsunami wave was recorded at 14.40 UTC at Kota Agung station, which was almost simultaneous with Cilegon station. Although Panjang is closer to Mount Krakatau Complex than Kota Agung, due to tsunami wave arrays that caused diffraction and refraction, the arrival time at Kota Agung was 10 minutes later than at Panjang stations (at 14.50 UTC). The landslide area at the southern part of Mount Anak Krakatau also contributed to arrival times.

Fig. 2. Filtered water elevation fluctuations measured at four tidal-gauge stations around Sunda Strait, indicating tsunami wave arrival times. Data was obtained from the Indonesia National Geospatial Information Agency (BIG, 2018).

4.2 Flow Depths and Inundation Area

Comparing the two main affected areas, a significant flow depth decay on both sides of the study areas was found. Highest flow depth was found at Cipenyu of Bantern, where the tsunami wave attacked directly from the area around Krakatau Complex. In the southern and the northern parts of this location, flow depth decreased. This was also found to be true in Lampung area. Detailed findings from both of these areas are elucidated as follows.

4.2.1 Banten

a. Serang District

Impacts of the tsunami in Banten were found to be more severe than in Lampung. Along the western coast of Banten, impacts were visible but not seen to be continuous. **Fig. 3** shows tsunami flow depth distribution and run-up limits measured at Banten coasts. There were some areas where evidence of tsunami waves could not be identified based on physical observations and eyewitness interviews. The northernmost extent of the tsunami effects was located at Anyar coast. The northernmost point of the tsunami depth was identified at a villa named Villa A Pahmi, located at Karang Suragak village. Here, the tsunami depth was 2.80 m (F02), identified from gazebo roof damage in the back yard of the villa.

Around this village, the maximum tsunami depth was 3.00 m (F01), based on a broken twig. Around Villa A Pahmi, a number of tsunami boulders were also found. Boulder materials came from a revetment structure protecting the coastline from erosion. Location of the revetment made determination of the travel distance of the transported boulders more facile. The farthest point of the transported boulder was

5   28 m from the revetment structure (Bo-1). Based on interviews with two tsunami survivors in this village, there were two significant wave attacks in this area; the second wave was the largest and the most destructive. A similar account was also revealed by another survivor at Villa Karang Bolong of Serang District. Tsunami waves damaged some houses and villas in this area. To the south of this area, impacts of the tsunami were more visible, as they were seen in Cinangka sub-district.

Fig. 3. Tsunami flow depth distribution around Serang, the northern area of Pandeglang district (left figure) and around southern Pandeglang area (Panimbang-Sumur, right figure). Flow depths are drawn in red bars. Green bars represent tsunami flow heights. The green rectangle represents the location of a

15   tsunami escape building at Labuan. (The map is adopted from Google Earth).

Fig. 4. A villa's wall destroyed by a tsunami in Bulukan Pondok beach (left) and a 2.08 m flow depth recorded on the stair inside the villa (right). A one-story house had major damage, while damage to the

20   two-story house was moderate.

At Cinangka sub-district, maximum tsunami flow depth was measured at 3.75 m (F25). This was identified from the peeled skin of a tree in Bulakan village. At Bulakan Pondok coast, in the same sub-

25   district, flow depth was measured at 2.08 m (F10), identified by a thick tsunami deposit at the stairway of a villa located about 12 m from coastline (see **Fig. 4**).

b. Pandeglang

30   Unlike Serang, where most of the coastal area is dominated by villas for tourism, Pandeglang's coastal area is mostly residential. Suka Ramai village, located at Sambolo Bay, was severely affected by the tsunami as can be seen from a cross profile of tsunami height and aerial images in Figs. 5 and 6. Tsunami wave direction is marked with a white arrow in the figure. Direction was identified from the direction of the fallen trees, swept away by the tsunami wave. At this location, tsunami flow depth was at 4.10 m

35   (F16) based on a broken tree branch. A higher flow depth was at 4.85 m at point F20 (Appendix).

At this location, a transect was performed to measure tsunami height. **Fig. 5** also shows the profile of tsunami flow heights, ground elevations and house damage type. Height was calibrated with local tide data. Here, the tsunami flow's height was 6.59 m (H1). As the crown of a seawall along this coastline

40   was 1.80 above mean sea level, the tsunami wave was considered significantly large enough to destroy

houses and other types of buildings in the area. Tsunami inundation distance reached 249 m, overpassing a dense residential area.

Fig. 5. A cross profile of tsunami height in Suka Ramai, Carita of Banten.

Further damages were identified in the Carita area of Pandeglang. The survey team investigated Mutiara Carita Cottage and Gading Nirwana Villa. The two resort complexes are situated close to the coastline and some of the buildings directly face the sea. Most of the buildings in this area were located about 15 m from the coastline, and apparently were not constructed for mitigating any waves coming from the

10   strait. Most of the buildings were flattened by the tsunami wave, leaving only floors. Based on a wall clock found at an inundated house, the clock stopped at 09.45 PM local time (14.45 UTC). At Mutiara Carita, measured tsunami flow depth was 3.50 m, identified by a broken tree branch, and 3.34 m, which was identified from a broken roof element of the cottage. These are Point F33 and F34 in the Appendix. A higher tsunami flow depth was found at Gading Nirwana Villa, which was 5.50 m (point F36). Flow

15   depth was identified from a broken roof at the villa. An aerial view of the cottage captured on 25 December 2019 can be seen in **Fig. 6**.

To the south of Carita, tsunami impacts were to be inconsistent in terms of distribution and depth. This was shown at Labuan, a fishermen's village, where the highest tsunami flow depth was 1.10 m, measured at Labuan Fishery port (PPP Labuan, Point F39 in the Appendix). A lower flow depth was also measured

20   at Lada bay of Panimbang sub-district, where the tsunami wave only overtopped a seawall structure and flooded a road behind the seawall. The crest of the seawall was about 1.50 m above ground elevation.

Interestingly, tsunami flow depths were found to be higher at Tanjung Jaya village than at Labuan. The village is located to the south of Labuan. In this village, there is also a Special Economic Zone (*KEK*),

25   where some industrial complexes are situated along with a resort (Tanjung Lesung resort). At this resort, a significant number of human casualties were identified. This was because there was a company family gathering where a popular musical band was performing at the time of the tsunami. According to an interview with the resort manager, the first tsunami wave attacked this resort at 09.30 PM local time (14.30 UTC). The first wave destroyed the performance stage, captured by amateur video recorded by a

30   party attendant. When this survey was conducted in this area, the broken stage was still visible and scattered. Here, flow depths were measured at 4.80 m and 4.95 m around the stage (Points F44 and F45, in the Appendix, respectively). Further landward, a flow depth as high as 2.30 m (F46) was still identified at about 120 m from the stage.

35   **Fig. 6.** Aerial view of land destruction at Mutiara Carita Cottages and Gading Nirwana Villa, Banten.

Fig. 7. Land destruction and flow depth distribution in Cipenyu Beach, Banten. Arrow shows direction of movement of the tsunami boulder transported by the wave.

Fig. 7 shows conditions at Cipenyu coast, located west of Tanjung Lesung resort, comparing scenes before and after the tsunami. The figure also shows the distribution of tsunami flow depths. Although no significant residential area was found here, traces of the massive impacts of the tsunami could be identified at Kasvana Beach Resort. Maximum flow depths around this resort were at 6.60 m (F47), identified from a broken branch of a *Pandanus Odorifer* sp. tree. According to an interview with the resort staff, seven people died. They were guests and staff of the resort. Severe erosion was also seen along the coastline near the resort. The deadly force of the tsunami wave was also revealed by a large tsunami boulder (Bo-5), which was found around 87 m from its initial source (see **Fig. 8**). The boulder's origin was based on eyewitness interviews stating that the boulder was at the beach area close to the resort before the tsunami. Another tsunami flow depth's mark close to the boulder was measured at 5.10 m (Point F54 in the Appendix). The topography around the area was relatively flat. Based on eq (1), it is inferred that the minimum velocity that transported the boulder was about 4.37 m/s.

At Sumur, to the southwest of Cipenyu, another zone of significant damage was observed. Although the population is lower than it is to the north of this area, visible tsunami traces could be identified from uprooted trees and fallen electrical poles. A steep coastal slope made it easier to locate tsunami flow depths and the limit of the tsunami inundation. Maximum run-up in this area was measured at 14.90 m from mean sea level. Maximum run-up was identified from debris apparently carried by the tsunami flow. At Cisiih village, the flow depth was measured at 5.85 m (Point F59 in the Appendix)

Sumur sub-district was the most affected sub-district at the southern part of Banten coast. This sub-district was isolated for about three days after the tsunami due to massive damage to roads and bridges connecting the sub-district to other areas. According to interviews with eyewitnesses, they experienced two tsunami waves where the second wave was the largest and the most destructive one. Before the first wave, residents heard a roaring sound from the sea that motivated most of the them to evacuate to higher ground. The residential area in this sub-district is situated very close to the sea. Some of the houses were located immediately behind a seawall. Tsunami flow depth was measured at 4.75 m from ground level (Point F60 in the Appendix). This point is located about 40 m from the seawall. A higher tsunami flow depth, measured at 5.25 m (F61), was also found in this sub-district. Most houses in this area were semi-permanent-type houses, where impacts of the tsunami waves on the houses were severe. Tsunami inundation limit was measured at 155 m from the coastline.

After Sumur, a survey was performed at Kertajaya sub-district, which was the last survey area in Banten. Tsunami impacts were investigated carefully at Cinibung resort. Here, flow depths were between 2.25 m–3.15 m. The survey at Banten area was completed on 30 December 2018, eight days after the tsunami.

Fig. 8. The largest boulder found in Cipenyu Beach-Banten was transported about 87 m from its original place. Arrow shows the estimated transport direction of the boulder with an estimated velocity of 4.37 m/s.

4.2.2 Lampung

a. South Lampung district

Impacts of the tsunami generated by the Mount Anak Krakatau eruption in Lampung Province were measured three locations, i.e. two areas in South Lampung and one area in Tanggamus District. South Lampung was the most tsunami-affected area at the Lampung coasts. In South Lampung district, impacts of the tsunami were found to be significant in Kalianda and Rajabasa sub-districts. Three villages in Kalianda were selected for detailed investigations, namely Way Kiayi, Way Urang and Maja. Distributions of tsunami flow depths in Kalianda can be seen in **Fig. 9**. In general, the majority of the Way Kiayi coastal residential community was deserted. Although tsunami flow depth was as high as 2.00 m and could still be found at an area about 100 m from coastline, not much major damage to buildings was identified. Nonetheless, some houses that were located around the coastal area were demolished by the tsunami wave, leaving floors as the only visible elements of the houses remaining. In Way Urang village, some houses were completely destroyed by the tsunami. A tsunami flow depth of 3.90 m was measured by one broken tree branch in the coastal area (Point F78 in the Appendix).

Maja Village's coastal area is a residential fishing village. A seawall was constructed to protect the houses from high waves generated from the Sunda Strait. Highest tsunami flow depth was 2.0 m from ground level (F70 and F71), measured at a house close to the seawall.

Impacts of the tsunami on Rajabasa area were worse than in Kalianda. We surveyed three villages in this sub-district, namely Way Muli, Kunjir and Batu Balak villages. Measured tsunami flow depths in this area were between 2.0 m–4.5 m as can be seen in **Fig. 10**. This is a fishing community, and the majority of the coastal area is a residential area for the fishermen. Other related buildings, such as a shrimp hatchery, were also damaged by the tsunami.

Fig. 12 shows an aerial view of the damage caused by the tsunami in Batu Balak and Kunjir villages. At the hatchery plant, tsunami flow depth was measured at 3.82 m from ground level (Point F88 in the Appendix). An elementary school in Kunjir located close to the coastline sustained massive damage. At this school, tsunami flow depth was measured at 3.33 m (Point F91). The tsunami inundation limit was located 160 m from the coastline. Although Kunjir area was protected by a revetment structure with a crown 2.5 m above mean sea level, it could not protect the area from the tsunami. On the revetment, tsunami flow depth was at 2.10 m, based on a tree mistakenly grown on top of the structure. In Way Muli, the highest tsunami flow depth was 3.92 m (Point F105).

Fig. 9. Flow depth distribution and run-up limits in Kalianda, South Lampung. Green bars and yellow triangles represent flow heights and inundation limits measured at the locations, respectively. (The map is adopted from Google Earth).

Fig. 10. Flow depth distribution and run-up limits in Rajabasa, South Lampung. (The map is adopted from Google Earth).

Fig. 11. Tsunami flow depth distribution in Kiluan Bay, Lampung. Dashed arrow represents the tsunami wave direction reflected from the closed end of the bay. (The map is adopted from Google Earth).

b. Tanggamus District

At Tanggamus District, Lampung, impacts of the tsunami were less severe. The only place where a casualty was reported was at Kiluan Bay of Kelumbayan sub-district. This bay is located about 79 km to the west of Bandar Lampung, the capital city of Lampung Province. Distribution of flow depths and flow directions at Kiluan Bay of Tanggamus can be seen in **Fig. 11**. Along the bay, there are three villages where tsunami impact was measured, namely, Sinar Agung, Sinar Maju and Bandung Jaya. Measured tsunami flow depths were 1.46 m, 1.15 m and 1.84 m at Sinar Agung, Sinar Maju and Bandung Jaya villages, respectively (see Points F114, F111 and F116 in the Appendix). The most severe impact in this area was investigated at a wooden elevated house that was transported about 3.5 m from its original location. The lone casualty was found at this location. Here, tsunami flow depth was 1.05 m (Point F115). Other damage was found at an elevated wooden house at the northeastern part of the bay. Based on eyewitness interviews, damaged was caused by the reflected tsunami wave after hitting the closed end of the bay.

Fig. 12. Tsunami-affected area around Batu Balak and Kunjir villages, Lampung.

4.3 Building Damages

Most buildings in the surveyed areas can be classified into two types, namely, confined masonry and wood. Wall components were brick. Roofs were wooden-framed with either tiled or zinc roofing. Detailed investigation of building damage was performed at 98 sites including the remaining houses and one school. Seventy-three of them were non-engineered, lightly reinforced concrete houses or confined masonry (CM), and 25 were wooden timber. There were 16 CM-type houses as classified by DS0. Impacts of tsunami debris were minor at houses near the coastline. Some tsunami debris was found to have contributed to house damage although most of the CM-type houses were mostly unaffected. Large debris was found at hotel complexes in Banten, where cars were carried by the tsunami flow and stopped by vegetation around the complexes. Damage to CM walls was mostly due to impulse or punching force produced by the tsunami flow. Unlike cases with tectonic events, shear-cracks on walls due to lateral forces were not found. Damage to columns was observed as collateral failure of walls combined with impacts of hydrodynamic forces. **Fig. 13** shows completely destroyed houses (DS4), where their types and material composition were known; these were also directly within tsunami flow depths as measured around the houses. Due to the limited number of surveyed houses, the fragility function was analysed using CM-type houses. A summary of the fragility functions analysis is given in **Table 2**. Fragility curves for all four types of damage can be seen in **Fig. 14**.

Table 2. Summary of damage to CM-type houses due to impacts of the 2018 Mount Anak Krakatau tsunami.

Fragility curves in **Fig. 14** reveal that the absolute damage due to the tsunami waves occurred at a flow depth of 6.5 m. Lower probabilities of complete damage were found in this study compared to the 2004 Indian Ocean tsunami in Banda Aceh (Koshimura et al., 2009). These findings were significantly
5   different from the 2018 Palu tsunami (Paulik et al., 2019) where earthquake and liquefaction (liquefied gravity flows) also contributed to the damage (Sassa and Takagawa, 2019).

There were 25 wooden houses surveyed in the affected area. Due to the limited number of surveyed wooden houses, analysis of the damage was performed by classifying the damage as seen in Table 1.
10   Only three classifications of damage could be identified, namely, DS2, DS3 and DS4. Two houses could be classified as DS2, seven houses were DS3, and 19 houses were DS4. Examples of the damage found at wooden houses due to tsunami impacts can be seen in **Fig. 13**. Based on the number of surveyed wooden houses, it was found that a tsunami flow depth higher than 2.0 m could completely wash away the houses, provided there was no debris in the flow. If the tsunami flow contained debris, the limit of
15   the tsunami flow depth that could wash away a house was lower. In cases where the flow depths were lower than 2.0 m, damage was found to be due to failure of the bottom plates of the walls. Similar investigations of the impacts of tsunami bores on wooden walls were completed by Linton et al. (2013) and Wilson et al. (2009). They revealed that (1) the tsunami flow at the foundations beneath the walls could generate an uplifting force, and (2) if the wave broke near the wooden structure, it also increased
20   loading. Although the location of the tsunami breaking wave in the 2018 Mount Anak Krakatau tsunami remains unknown, the pattern of damage to the lower parts of the wooden walls were similar to those in these studies.

25   **Fig. 13**. Examples of damage to wooden houses: (a) major damage and (b) complete damage/washout.

Fig. 14. Fragility curves of confined masonry-type houses, for impacts of the 2018 Mount Anak Krakatau volcanogenic tsunami. Dashed line represents a complete damage fragility curve produced by Koshimura et al. (2009).)

5 Discussions

5.1 Flow depths and arrival time

In Banten, tsunami flow depths were found to be higher than those measured in Lampung on the Sumatra side. Although Mount Anak Krakatau is nearly equidistant to the Lampung and Banten coasts, flow depths were apparently higher in Banten. Furthermore, impacts of the tsunami were more severe on the Banten coasts. As the event was caused by a non-tectonic process at night, a large number of people fell
40   victim to the unavailability of tsunami warnings that could have anticipated a volcanogeneric tsunami. Significant flow depth decay found in this study was similar to that found during the 2002 Stromboli tsunami as these were typical landslide-tsunamis (Tinti et al., 2006; Okal and Synolakis, 2003).

The volcanogenic tsunami is a discernible event. There have been hundreds of tsunami events recorded in Indonesia since the 16th century, with only 11% generated by a volcanic eruption (Latief et al., 2000; Puspito and Gunawan, 2005; Lovholt et al., 2012; Pribadi et al., 2013). The 22 December 2018 Sunda
5 Strait tsunami was an apparent unanticipated event caused by the southwest flank failure of Mount Anak Krakatau. There was no proper warning released by the authorities as the present tsunami warning system cannot anticipate non-tectonic tsunamis as in the case of the 2018 Sunda Strait tsunami. Furthermore, tsunami arrivals were presumably on short notice. As in the case of the 2002 Stromboli volcano tsunami, arrival times were six minutes at a distance similar to that of the 2018 Mount Anak Krakatau tsunami
10 (Bonaccorso et al., 2003). This problem was evident during the 28 September 2018 tsunami event (Syamsidik et al., 2019; Takagi et al., 2018). Following the 2018 Mount Anak Krakatau tsunami, the Government of Indonesia has been planning to install a number of tidal gauges to monitor water elevation around the volcano complex associated with tsunami wave generation. Nonetheless, it should be noted that, despite the installations, it will still be difficult to detect tsunami waves with this method without
15 other supporting sensors. This was proven in the case of Mount Stromboli in Italy (Tinti et al., 2003).

To anticipate tsunamis at the Banten coasts, there is one official escape building in Labuan. It is located about 420 m from the coastline. During the 22 December 2018 event, this building was used by the community as a shelter, despite its being far from the affected area. Labuan Port was hit by a tsunami
20 wave at 1.10 m. There were no major damages found at this location. The location of the tsunami escape building in Labuan needs to be reconsidered, and further steps are required to properly accommodate the tsunami evacuation process. Lessons learned from tsunami escape buildings in Aceh and coastal settlements after the 2004 Indian Ocean tsunami should be taken into account (see McCaughey et al., 2017; Syamsidik et al., 2017).

5.2 Characteristics of Building Damage

Damage to buildings and houses was more severe in Banten than in Lampung. Most of the damages were
30 found in wall components. As a majority of buildings in Banten and Lampung were constructed with brick walls, the masonry-infill walls had a 50 % probability of damage when tsunami flow depth reached 2.3 m, and would certainly have experienced major damage when the flow depth reached 5.05 m. Unlike damage found in the cases of tectonic tsunamis, diagonal cracks in the buildings resulting from lateral forces were not found. The CM-type house would be completely washed away by the tsunami when flow
35 depth reached 6.6 m. These findings demonstrated a slightly different pattern compared to tectonic tsunamis (Koshimura et al., 2009, Paulik et al., 2019). It is worth noting that the latter two studies examined a combination of tectonic and tsunami forces. Damage could even start when the flow depth has yet to reach its maximum level (Suppasri et al., 2019). A lower flow depth that could cause complete damage to the CM-type house was shown by Shoji et al. (2014). However, this was a non-probabilistic
40 study with only 25 sample houses observed. In the case of the 2018 Mount Anak Krakatau tsunami, the

wavelength could have been shorter as this was similar to a landslide-driven tsunami. This would have generated a smaller impulsive force on buildings. Therefore, this could also be a further explanation for the difference in fragility curves derived from the 2004 Indian Ocean tsunami compared to the 2018 Mount Anak Krakatau tsunami.

No building was overturned by the tsunami wave as in the case the 2011 Great East Japan earthquake and tsunami (Yeh et al., 2013; Latcharote et al., 2014). This proved that the damage to the buildings was generally due to impact and drag forces. Debris-laden flow forces did not impact most of the damaged houses located close to the coastline. Hydrodynamic forces decreased as the speed of the wave decreased

10   due to the roughness coefficient of the land use types (Saatçioğlu et al., 2006). A specific case was found at Mutiara Carita Cottages (see **Figs. 5** and **6**). Here, the force became larger when gaps between buildings were smaller. This was also found in some cases in Banda Aceh during the 2004 Indian Ocean tsunami (Triatmadja and Benazir, 2014). Debris generated mostly by the fronts of buildings facing the tsunami wave caused severe damage to other buildings downstream of the tsunami flow.

5.3 Limitations of the study

Limitations of this study lay within several aspects. The first limitation was that the time of the tsunami generation from the Mount Anak Krakatau was still unknown when this article was submitted. There was

20   no tidal gauge or sensor placed around the volcano complex that could have detected the first generation of the tsunami wave near the source. The second limitation was that the volcanic mechanism that generated the tsunami is still not known. There are four mechanisms that could have potentially generated the tsunami, such as underwater explosion, flank failures (landslide), pyroclastic flow and volcano crest collapse. The most likely process that generated the 2018 Mount Anak Krakatau tsunami was the latter

25   one. This is based on aerial images captured before and after the tsunami. However, whether other mechanisms could also have contributed to the tsunami could not be verified as of this publication. The third limitation was that estimation of the velocity was based on tsunami boulder transport, whereas the calculation was based on experimental formulae. This would result in an estimated tsunami velocity rather than a recorded velocity. Tsunami fragility curves were drawn based on a limited number of

30   tsunami-affected houses. Additional explanation and figures from the surveys can be found in TDMRC (2018; 2019). Notwithstanding these limitations, this study conclusively revealed the impacts of a pure tsunami wave force on buildings and could be useful for further studies in tsunami engineering and mitigation.

35   ## 6   Conclusions

The 2018 Mount Anak Krakatau tsunami provided new insights into tsunami damage mitigation. This study was mostly based on a series of field surveys to investigate the impacts of the 2018 Mount Anak Krakatau tsunami on two major affected areas, i.e., Banten and Lampung on the western Java coasts and

southern Sumatra coasts, respectively. Starting the 10-day survey just two days after the tsunami offered the team a better opportunity to collect undisturbed tsunami evidence. Study conclusions are as follows:

a. Tsunami flow depths were found to be relatively higher at Banten area than at Lampung. Arrival times were slightly faster in Banten than on the Lampung side although it is important to note that the initial time of tsunami wave generation from the source is still unknown. Maximum velocity was about 4.37 m/s, inferred from a tsunami boulder measured at Banten. Highest tsunami flow depth was 6.6 m, also measured on the Banten side.

b. Impacts of the tsunami on houses were inferred from fragility functions derived from CM type houses. These houses had a 50% probability of being washed away by the tsunami if the tsunami flow depth had reached 4.5 m. Furthermore, had the tsunami depth reached 2.3 m, the houses would have had a 50% probability of sustaining major damage. Wooden houses were likely to be completely damaged by the tsunami if the flow depth were higher than 2.0 m.

c. Evacuation of the coastal community during the tsunami was difficult as there was not a proper warning released before the first wave attacked the area. The only sound that saved some people in Sumur of Banten was a roaring sound coming from the Sunda Strait. Modification and enhancement of tsunami early warnings are required in order to anticipate a volcanogenic tsunami in the future as Mount Anak Krakatau should remain active and pose threats to the surrounding area.

As a majority of the houses in the coastal areas of Indonesia are CM, it is highly recommended to increase quality control of these structures, such as in the bounding strength between walls and tie-beams or tie-columns. In the case of purely tsunami force, this type of structure would likely perform better if stricter quality standards are met.

Acknowledgements

We gratefully thank to *Partnership Enhanced Engagement in Research (PEER)* Cycle 5 sponsored by the United States Agency for International Development (USAID) and National Academies of Sciences, Engineering, and Medicines of United States (NASEM) under research grant #5-395, title *Incorporating climate change induced sea level rise information into coastal cities' preparedness toward coastal hazards* with Sponsor Grant Award No. AID-OAAA-A-11-00012 and Subaward No. 2000007546. A visit of Prof. Anawat Suppasri (co-author of this article) to Banda Aceh and paper fine-tuning activities were performed under the World Class Professor Program (WCP) Scheme B, promoted by Ministry of Research, Technology, and Higher Education of Indonesia (KEMENRISTEKDIKTI) in 2019 (Contract No. T/80/D2.3/KK.04.05/2019). At the same time, the first author would like to thank to Prof. Fumihiko Imamura, the Director of International Research Institute of Disaster Science (IRIDeS) of Tohoku University for facilitating the writing residency program for the completion of this paper.

References

Bani, P., Normier, A., Bacri, C., Allard, P., Gunawan, H., Hendrasto, M., Surono, and Tsanev, V., 2015.
5   First measurement of the volcanic gas output from Anak Krakatau, Indonesia. Journal of
       Volcanology and Geothermal Research 302, 23-241.

BIG (Indonesia National Geospatial Information Agency), 2018.
       http://tides.big.go.id:8888/dash/ (2018), Accessed on 23rd December 2018

Boen, T., 2005 Sumatra Earthquke Dec 26 2004. Earthquake Engineering Research Institute.
10   California, USA.
       https://www.eeri.org/~eeriorg/lfe/clearinghouse/sumatra_tsunami/reports/Boen_Sumatra%20Eart
       hquake%2026%20Dec%202004.pdf (accessed on June 20, 2019).

Bonnaccorso, A., Calvary,S., Garfield, G., Lotado, L., and Patane , D., 2003. Dynamics of the
       December 2002 flank failure and tsunami at Stromboli volcano inferred by volcanological and
15   geophysical observations. Geophysical Research Letters, 30(18), 1941.

Borrero C. Jose, Costas E. Synolakis, and Hermann Fritz (2006) Northern Sumatra Field Survey after
       the December 2004 Great Sumatra Earthquake and Indian Ocean Tsunami. Earthquake Spectra:
       June 2006, Vol. 22, No. S3, pp. 93-104.

Brzev, S., 2007. Earthquake-resistant confined masonry construction. Master Thesis. British Columbia
20   Institute of Technology, Burnaby. Canada.

Choi, B.H., Pelinovsky, E., Kim, K.O., and Lee, J.S., 2003. Simulation of the trans-oceanic tsunami
       propagation due to the 1883 Krakatau volcanic eruption. Natural Hazards and Earth System
       Sciences 3, 321-332.

Deblus, C., Bonvalot,S., Dahrin, D., Diament, M., Harjono, H., and Dubois, J., 1995. Inner structure of
25   the Krakatau volcanic complex (Indonesia) from gravity and bathymetry data. Journal of
       Vulcanology and Geothermal Research, 64, 23-52.

Donovan, A., Suppasri, A., Kuri, M., and Torayashiki, T., 2018. The complex consequences of
       volcanic warnings: Trus, risk perception and experiences of businesses near Mount Zao following
       the 2015 unrest period. International Journal of Disaster Risk Reduction, 27, 57-67.

30 EERI (Earthquake Engineering Research Institute), 2006. Special Issue on the Great Sumatra
       Earthquakes and Indian Ocean Tsunamis of 26 December 2004 and 28 March 2005. Earthquake
       Spectra, 22, No S3.

Emery, W.J. and Thomson, R.E., 2001. Data Analysis Methods in Physical Oceanography. Elsevier,
       Amsterdam. https://doi.org/10.1016/B978-0-444-50756-3.X5000-X.

35 Fryer, G.J., 2011. Walk the inundation limit: A suggestion for future post-tsunami surveys. Earth-
       Science Reviews 107, 123-127.

GVP   (Global   Volcanism   Program),   2019.   Krakatau,   Eruptive   History.
       http://volcano.si.edu/volcano.cfm?vn=262000 (accessed on February, 2019).

Gerard J. Fryer, Walk the inundation limit: A suggestion for future post-tsunami surveys, Earth-Science Reviews, Volume 107, Issues 1–2, 2011, Pages 123-127, https://doi.org/10.1016/j.earscirev.2011.03.003.

5 Giachetti, T., Paris, R., Kelfoun, K., and Ontowirjo, B., 2012. Tsunami hazard related to a flank collapse of Anak Krakatau Volcano, Sunda Strait, Indonesia. Terry, J. P. & Goff, J. (eds). Natural Hazards in the Asia–Pacific Region: Recent Advances and Emerging Concepts. Geological Society, London, Special Publications, 361, 79–90, http://dx.doi.org/10.1144/SP361.7

Jaffe, B.E., Gelfenbaum, G., Buckley, M.L., Watt, S., Apotsos, A., Stevens, A.W., Richmond, B.M., 2010. The limit of inundation of the September 29, 2009 tsunami on Tutuila, American Samoa. 10 U.S. Geological Survey Open-File Report 2010-1018. 27p.

Koshimura, S., Oie, T., Yanagisawa, H., and Imamura, F., 2009. Developing fragility functions for tsunami damage estimation using numerical model and post-tsunami data from Banda Aceh, Indonesia. Coastal Engineering Journal 5(13), 243-273.

Latcharote, P., Suppasri, A., Yamashita, A., Adriano, B., Koshimura, S., Kai, Y., and Imamura, F., 15 2017. Possible failure mechanism of buildings overturned during the 2011 Great East Japan tsunami in the town of Onagawa. Front. Built Environ, 3,16, DOI: https://doi.org/10.3389/fbuil.2017.00016.

Latief, H., Puspito, N. T. & Imamura, F., 2000. Tsunami Catalog and Zones in Indonesia. Natural Disaster Science, Volume 22, pp. 25-43.

20 Linton, D., Gupta, R., Cox, D., van de Lindt, J., Oshnack, M.E., and Clauson, M., 2013. Evaluation of tsunami loads on wood-frame walls at full scale. Journal of Structural Engineering, J. Struct. Eng., 2013, 139(8): 1318-1325. DOI: 10.1061/(ASCE)ST.1943-541X.0000644.

Løvholt, F. et al., 2012. Historical Tsunami and Present Tsunami Hazard in Eastren Indonesia and The Southern Philippines. Journal of Geophysical Research, Volume 117.

25 Macabuag, J., Rosetto, T., Ioannou, I., Suppasri, A., Sugawara, D., Adriano, B., Imamura, F., Eames, I., and Koshimura, S., 2016. A proposed methodology for deriving tsunami fragility functions for buildings using optimum intensity measures. Natural Hazards, 84(2), 1257-1285.

McCaughey, J.W., Mundir, I., Daly, P., Mahdi, S., Patt, A., 2017. Trust and distrust of tsunami vertical evacuation buildings: extending protection motivation theory to examine choices under social 30 influence. International Journal of Disaster Risk Reduction, 24, 462-473. DOI: https://doi.org/10.1016/j.ijdrr.2017.06.016.

Nandasena, N.A.K., Paris, R., and Tanaka, N., 2011. Reassessment of hydrodynamic equations: Minimum flow velocity to initiate boulder transport by high energy events (storms, tsunamis). Marine Geology, 281(1-4), 70-84.

35 Noormets, R., Crook, K.A.W., Felton, E.A., 2004. Sedimentology of rocky shorelines: 3. Hydrodynamics of megaclasts emplacement and transport on a shore-platfomr, Oahu, Hawai. Sedimentary Geology, 172, 41-65.

Okal, E.A. and Synolakis, C.E., 2003. A theoretical comparison of tsunamis from dislocations and landslides. Pure Appl Geophys, 160, 2177–2188. https://doi.org/10.1007/s00024-003-2425-x

PVMBG (Center of Volcanology Survey of Indonesia), 2018. Pers Release on Activit of Mount Anak Krakatau. http://www.vsi.esdm.go.id/index.php/gunungapi/aktivitas-gunungapi/2567-pers-rilis-aktivitas-gunungapi-anak-krakatau-kamis-27-desember-2018

Paris, R., Fournier, J., Poizot, E., Etienne, S., Morin, J., Lavigne, F., and Wassmer, P., 2010. Boulder and fine sediment transport and deposition by the 2004 tsunami in Lhok Nga (western Banda Aceh, Sumatra, Indonesia): A coupled offshore-onshore model. Marine Geology 268, 43-54.

Paris, R., Wassmer, P., Sartohadi, J., Lavigne, F., Barthomeuf, B., Desgages, E., Grancher, D., Baumert, Ph., Vautier, F., Brunstein, D., and Gomez, Ch., 2009. Tsunamis as geomorphic crisis: lessons from the December 26, 2004 tsunami in Lhok Ng, west Banda Aceh (Sumatra, Indonesia). Geomorphology, 104, 59-72.

Paulik, R., Gusman, A., Williams, J.H, Pratama, G.M., Lin, S-L., Prawirabhakti, A., Sulendra, K., Zachari, M.Y., Fortuna, E.D., Layuk, N.B.P., and Suwarni, N.I.K., 2019. Tsunami hazard and built environment damage observations from Palu city after the September 28 2018 Sulawesi earthquake and tsunami. Pure and Applied Geophysics. https://doi.org/10.1007/s00024-019-02254-9

Pribadi, S., Afnimar, Puspito, N. T. & Ibrahim, G., 2013. Characteristics of Earthquake-Generated Tsunamis in Indonesia based on Source Parameter Analysis. J. Math. Fund. Sci, Volume 45 No. 2, pp. 189-207.

Puspito, N. T. & Gunawan, I., 2005. Tsunami Sources in The Sumatra Region, Indonesia and Simulation of The 26 december 2004 Aceh Tsunami. ISET Journal of Earthquake Technology, Volume 42 No. 4, pp. 111-125.

Saatçioğlu M., Ghobarah, A., and Nistor, I., 2006. Performance of Structures During the 2004 Indian Ocean Tsunami and Tsunami Induced Forces for Structural Design. Earthquake Spectra, 22(S3), S295-S319.

Sassa, S. and Takagawa, T., 2019. Liquefied gravity flow-induced tsunami: first evidence and comparison from the 2018 Indonesia Sulawesi earthquake and tsunami disasters. Landslide, 16, 195-200. DOI 10.1007/s10346-018-1114-x

Shoji, G., Shimizu, H., Koshimura, S., Estrada, M., and Jimenez, C., 2014. Evaluation of tsunami wave loads acting on walls of confined masonry-brick and concrete-block houses. Journal of Disaster Research, 9(6), 976-983. DOI: 10.20965/jdr.2014.p0976.

Sigurdsson, H., Carey, S. and Mandeville, C., 1991. Sub-marine pyroclastic flows of the 1883 eruption of the Krakatau Volcano. National Geographic Research and Exploration, 7: 3 10-327.

Suppasri, A., Charvet, I., Imai, K. and Imamura, F. , 2015. Fragility curves based on data from the 2011 Great East Japan tsunami in Ishinomaki city with discussion of parameters influencing building damage, Earthquake Spectra, 31 (2), 841-868.

Suppasri, A., Charvet, I., Kentaro, I., and Imamura, F., 2014. Fragility curves based on data from the 2011 Great East Japan tsunami in Ishinomaki city with discussion parameters influencing damage. Earth. Spectra 31(2), 841-868.

Suppasri, A., Pakoksung, K., Charvet, I., Chua, C. T., Takahashi, N., Ornthammarath, T., Latcharote, P., Leelawat, N., and Imamura, F.: Load-resistance analysis: An alternative approach to tsunami

damage assessment applied to the 2011 Great East Japan tsunami, Nat. Hazards Earth Syst. Sci. Discuss., https://doi.org/10.5194/nhess-2019-71,accepted, 2019.

Suppasri, A., Koshimura, S., and Imamura, F., 2011. Developing tsunami fragility curves based on the Satellite remote sensing and numerical modelling of the 2004 Indian Ocean tsunami in Thailand.

5   Natural Hazards and Earth System Sciences, 11(1), 173-189.

Syamsidik, Benazir, Umar, M., Margaglio, G., and Fitrayansyah, A., 2019a. Post tsunami survey of the 28 September 2018 tsunami near Palu bay in Central Sulawesi, Indonesia: Impacts and Challenges to Coastal Communities. International Journal of Disaster Risk Reduction 38, DOI: 10.1016/j.ijdrr.2019.101229.

10   Syamsidik, Benazir, and Luthfi, M., 2019b. Tsunami Flow Depths, Building Damages, and tsunami boulders Measured from the December 22, 2018 Sunda Strait Tsunami around Western Java and Southern Lampung of Indonesia. Mendeley Data. http://dx.doi.org/10.17632/yyyvmxh8vg.1

Syamsidik, Oktari, R.S., Munadi, K., Arief, S., and Fajri, I.Z., 2017. Changes in coastal land use and the reasons for selecting places to live in Banda Aceh 10 years after the 2004 Indian Ocean

15   tsunami. Natural Hazards, 88(3), 1503-1521. DOI: https://doi.org/10.1007/s11069-017-2930-3.

TDMRC (Tsunami and Disaster Mitigation Research Center), 2018. The 2018 Sunda Strait Tsunami Impacts Assesment. Universitas Syiah Kuala, Banda Aceh-Indonesia. http://tdmrc.unsyiah.ac.id/the-2018-sunda-strait-tsunami-impacts-assessment/.

TDMRC (Tsunami and Disaster Mitigation Research Center), 2018. The latest update from post-sunda

20   strait tsunami survey. Universitas Syiah Kuala, Banda aceh-Indonesia. http://tdmrc.unsyiah.ac.id/the-latest-update-from-post-sunda-strait-tsunami-survey/.

Teresita, G., Nicola, M., Luca, F., and Pierfrancesco, C., 2019. Tsunami risk perception along the Thyrrhenian coasts of Souther Italy: the case of Marsili volcano. Natural Hazards. https://doi.org/10.1007/s11069-019-03652-x.

25   Tinti, S., Maramai, A., Armigliato, A., Graziani, L., Manucci, A., Pagnoni, G., Zaniboni F., 2006. Observations of physical effects from tsunamis of December 30, 2002 at Stromboli volcano, southern Italy. Bulletin Volcanology, 68(5), 450-461. https://doi.org/10.1007/s00445-005-0021-x.

Tinti, S., Pagnoni, G., Zaniboni, F., and Bortolucci, E., 2003. Tsunami generation in Stromboli island

30   and impact on the south-east Tyrrhenian coasts. Natural and Earth System Sciences, 3, 299-309.

Topex (Topogaphy Expriment of the Ocean), 2019. Extract xyz grid-topography or gravity. https://topex.ucsd.edu/cgi-bin/get (accessed on June 20, 2019).

Triatmadja, R. and Benazir, 2014. Simulation of tsunami force on rows of buildings in Aceh region after tsunami disaster in 2004. Science of Tsunami Hazard, 33(3), 156-169.

35   Williams, R., Rowley, P., and Garthwaite, M. C., 2019. Reconstructing the Anak Krakatau flank collapse that caused the December 2018 Indonesian tsunami. EarthArXiv. https://doi.org/10.31223/osf.io/u965c.

Wilson, J.S., Gupta, R.G., van de Lindt, J.W., Clauson, M., and Garcia, R., 2009. Behavior of a one-sixth scale wood-frame residential structure under wave loading. Journal of Performance of

40   Constructed Facilities, 23(5), 336-345. DOI: 10.1061/(ASCE)CF.1943-5509.0000039.

Yeh, H., Sato, S. & Tajima, Y. Pure Appl. Geophys. (2013) 170: 1019. https://doi.org/10.1007/s00024-012-0489-1.

Zen, M.T., 1970. Growth and state of Anak Krakatau in September 1968, Bull. Volcanol. 34 (1), 205–215.

Table 1. Damage states of buildings due to tsunami as suggested by Suppasri et al. (2011) and Macabuag et al. (2016).

Classification	Damage Condition	Description	An Example Photo
DC0	No damages	Flooded but no damages found.	
DC1	Minor	Damages found windows and doors, no damage on wall and on structural component	
DC2	Moderate	One side wall damages, no damage on column and beam.	
DC3	Major	All walls were damaged or roofs felt down, structural components bent/deflected or broken.	
DC4	Complete/Washed aw ay	Only floor left.	

Table 2. A summary of damage conditions of CM-type houses due to impacts of the 2018 Mount Anak Krakatau tsunami.

Damage Condition	Number of houses	μ	σ	R^2
DS0	14	-	-	-
DS1	4	1.1585	0.2848	0.999
DS2	8	1.6499	0.5249	0.898
DS3	32	2.2806	0.8021	0.877
DS4	13	4.5017	0.9195	0.894
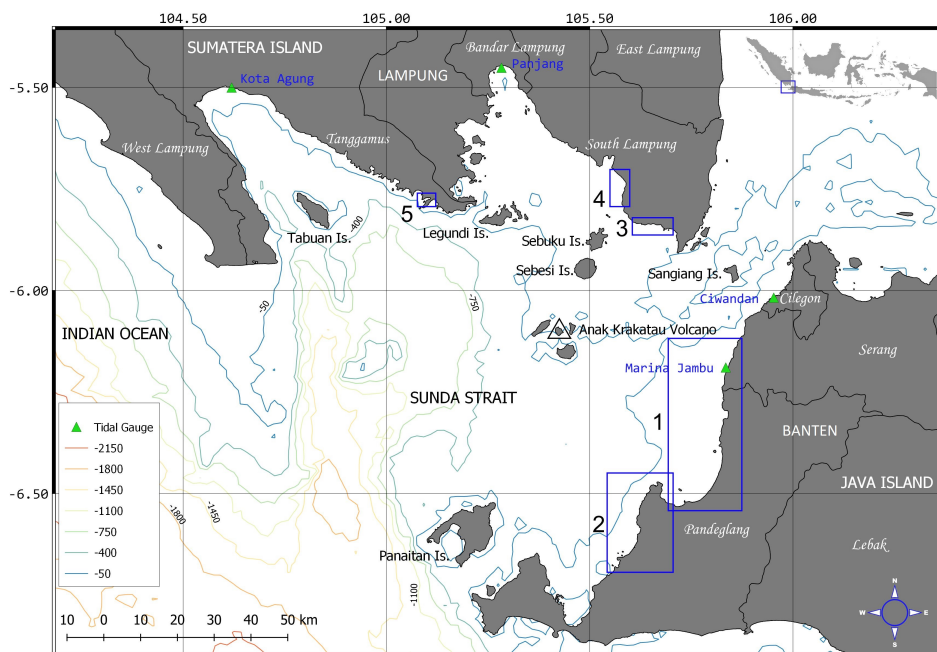
Fig. 1. The surveyed area following the December 22, 2018 Mount Anak Krakatau volcano-genic tsunami. Five areas of the survey are marked in blue-rectangular. Tide-gauge stations are marked in green triangles. Bathymetry data were adopted from Topex (2019).
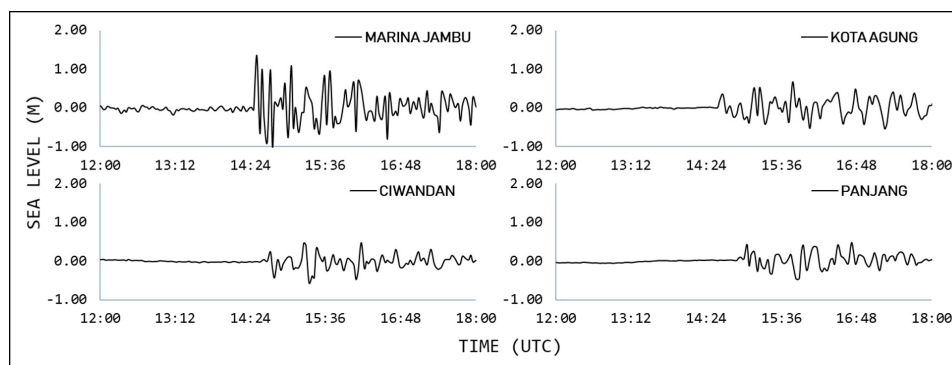
Fig. 2. Filtered water elevation fluctuations measured at four tide-gauge stations around Sunda Strait, indicating the arrival tsunami wave.
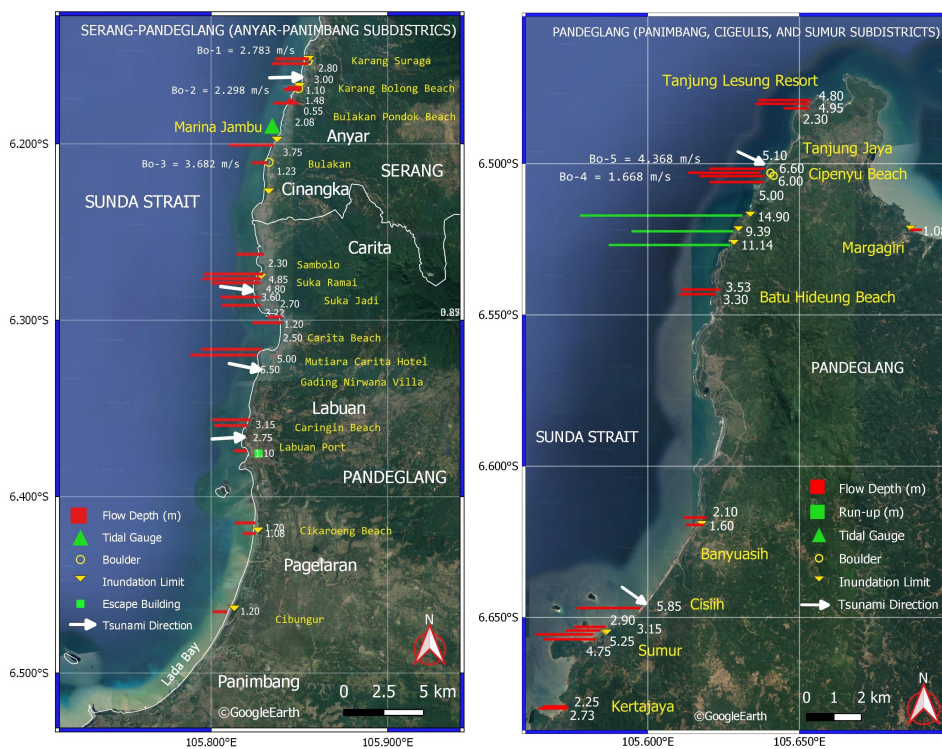
Fig. 3. Tsunami flow depths distribution around Serang and northern area of Pandeglang district (left figure) and around southern Pandeglang area (Panimbang-Sumur) (right figure). (The map is adopted from Google Earth).

Fig. 4. A villa's wall destroyed by tsunami in Bulukan Pondok beach (left) and a 2.08 m of flow depth recorded on the stair inside the villa (right). One story house had a major damage, meanwhile the two-storeys house was moderate.
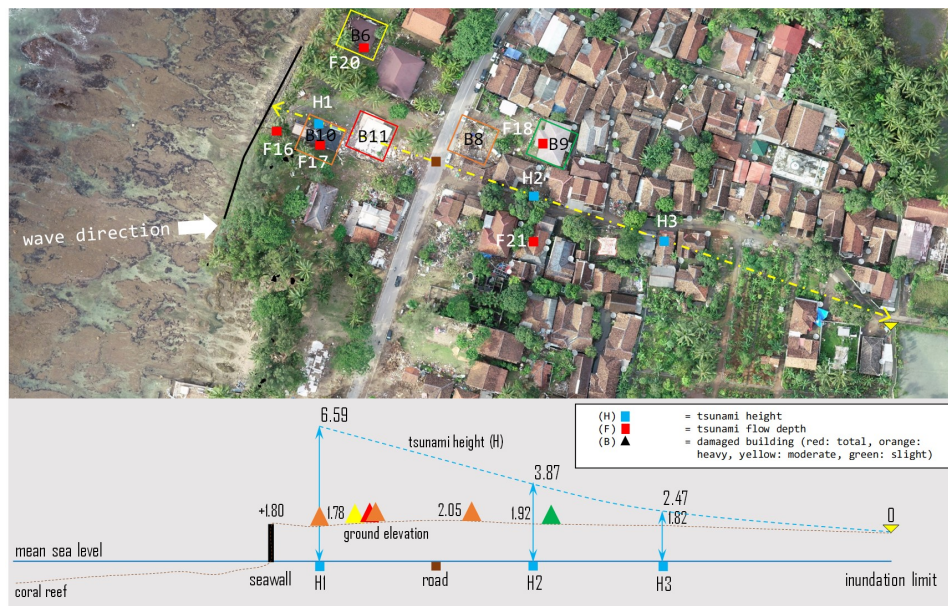
Fig. 5. A cross profile of tsunami height in Suka Ramai, Carita of Banten. The upper figure is the location of the transect plotted on an aerial image captured on December 28, 2018.

Figure 6. Aerial view of land desctruction in Mutiara Carita Cottages and Gading Nirwana Villa, Banten.

Fig. 7. The land destruction and flow depth distribution in Cipenyu Beach, Banten. Left hand-side photo is a google earth image captured before the tsunami (from © Google Earth). Right hand-side photo is an aerial view captured by drone on December 29, 2018.

Fig. 8. The largest boulder found in Cipenyu Beach, Banten; captured on December 28, 2018.
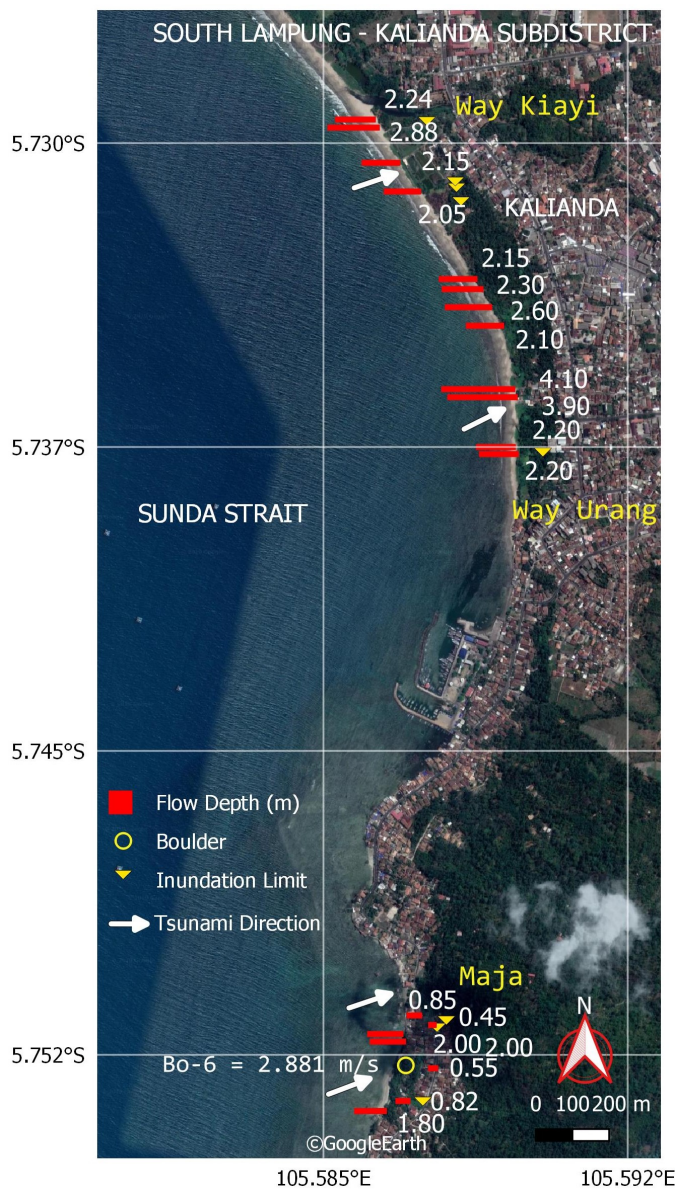
Fig. 9. Flow depths distribution and run-up limits in Kalianda, South Lampung. (The map is adopted from Google Earth).
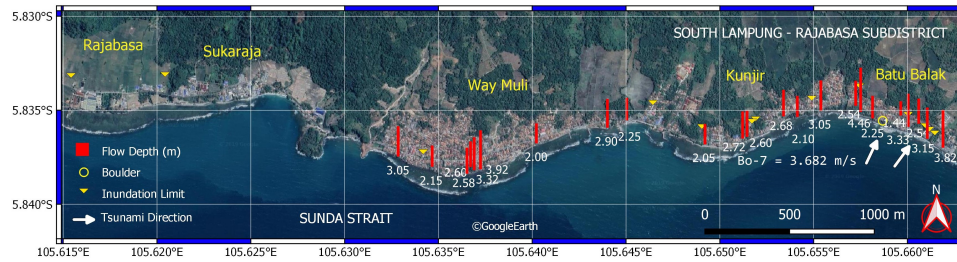
Fig. 10. Flow depths distribution and run-up limits in Rajabasa, South Lampung. (The map is adopted from Google Earth).
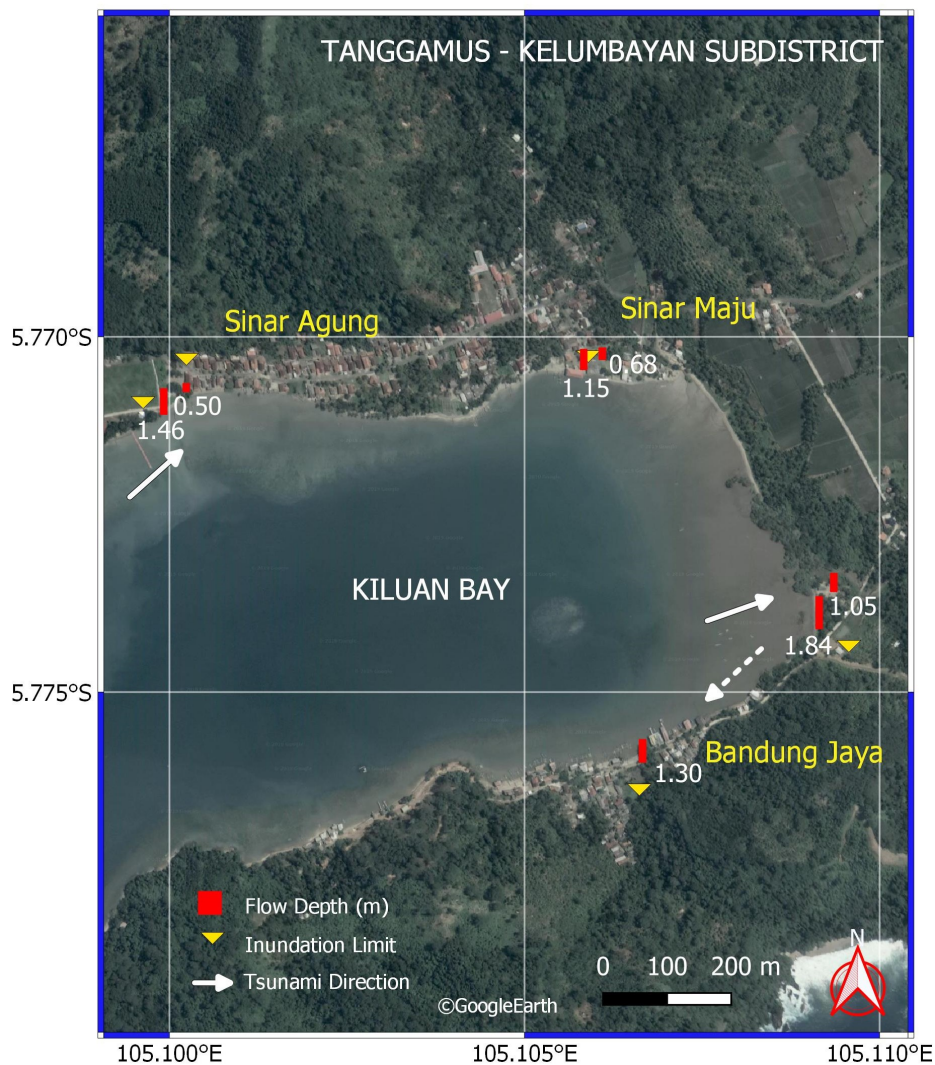
Fig. 11. Tsunami flow depths distribution in Kiluan Bay, Lampung. A dash-arrow represents the tsunami wave direction reflected from the close-end of the bay. (The map is adopted from Google Earth).
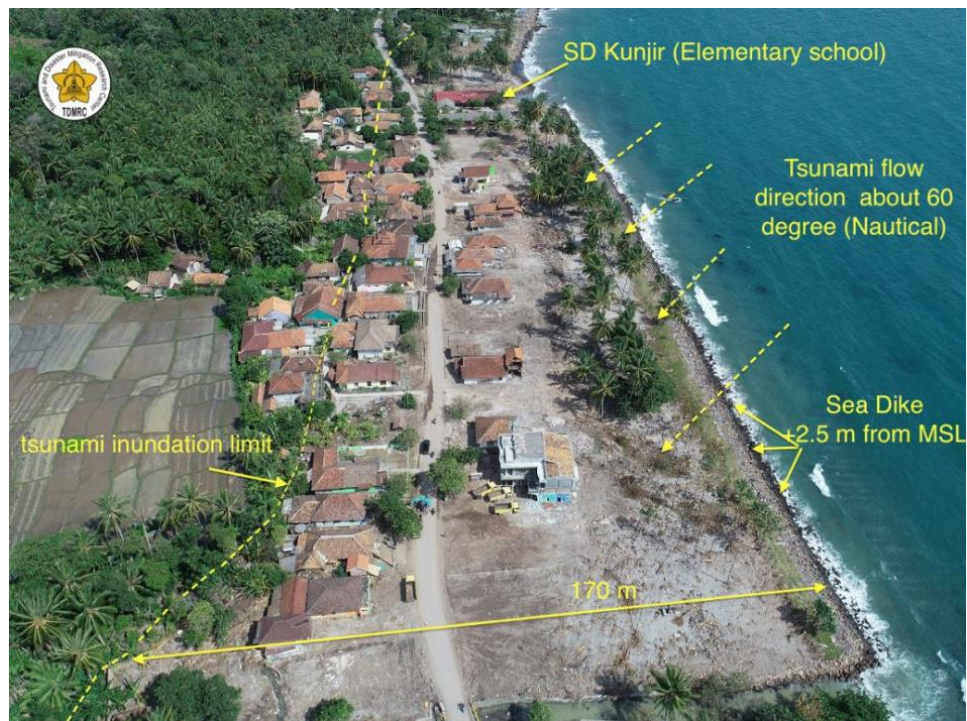
Fig. 12. An aerial view from tsunami-affected area around Batu Balak and Kunjir villages, Lampung, captured on
December 31, 2018.

Fig. 13. Examples of damages at wooden houses: (a) Major damages and (b) complete damage/washed away.
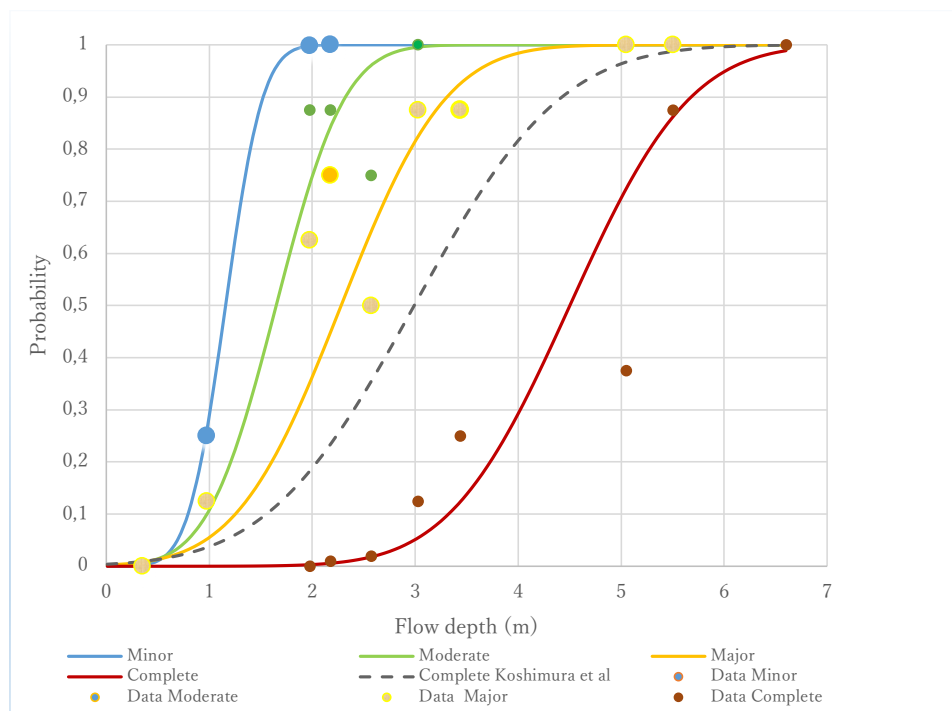
Fig. 14. Fragility curves of Confined Masonry type houses, as impacts of the 2018 Mount Anak Krakatau volcano-genic tsunami. Dashed-line represents a complete damage fragility curve produced by Koshimura et al. (2009).

APPENDICES

Appendix A. Tsunami Flow Depths

NO	ID	LON	LAT	FLOW DEPTH (M)	HEIGHT (M)	RUN-UP (M)	LOCATION	NOTE
1	F01	105.854735	-6.153396	3.00	-	-	Karang Suragak, Serang	Broken twig of a tree
2	F02	105.854688	-6.152983	2.80	-	-	Karang Suragak, Serang	Broken twig of a tree at A. Pahmi villa
3	F03	105.855002	-6.152984	0.50	-	-	Karang Suragak, Serang	Watermark on the wall of A. Pahmi villa
4	F04	105.849783	-6.168017	1.00	-	-	Karang Bolong Beach, Serang	Watermark on the wall of Karang Bolong villa
5	F05	105.849934	-6.168391	0.84	-	-	Karang Bolong Beach, Serang	Watermark on the wall of toilet's villa
6	F06	105.849930	-6.168480	1.02	-	-	Karang Bolong Beach, Serang	Watermark on the wall of prayer room's villa
7	F07	105.849609	-6.168915	1.48	-	-	Karang Bolong Beach, Serang	Watermark on the wall of a villa
8	F08	105.849742	-6.168791	1.10	-	-	Karang Bolong Beach, Serang	Scratch of bark of a tree near villa
9	F09	105.846891	-6.175977	0.55	-	-	Bulakan Pondok Beach, Serang	Watermark on the wall of a house
10	F10	105.846387	-6.175758	2.08	-	-	Bulakan Pondok Beach, Serang	Tsunami deposit (fine sand) on the villa's stairs
11	F11	105.827257	-6.288090	0.85	-	-	Suka Jadi, Pandeglang	Watermark on the wall of hencoop
12	F12	105.826556	-6.287863	3.27	-	-	Suka Jadi, Pandeglang	Debris (fresh twig) on a tree
13	F13	105.829244	-6.262511	2.30	-	-	Suka Ramai, Pandeglang	Scratch of bark of a tree
14	F14	105.827630	-6.290189	2.70	-	-	Suka Ramai, Pandeglang	Debris (fresh twig) on a tree
15	F15	105.827536	-6.290687	3.22	-	-	Suka Ramai, Pandeglang	Broken coconut midrib near shoreline
16	F16	105.826325	-6.276125	4.10	-	-	Suka Ramai, Pandeglang	Broken twig of a tree
17	F17	105.826398	-6.276132	4.80	-	-	Suka Ramai, Pandeglang	Broken roof tile of a house
18	F18	105.827170	-6.276110	1.95	-	-	Suka Ramai, Pandeglang	Watermark on the wall of a house
19	F19	105.827204	-6.276455	1.00	-	-	Suka Ramai, Pandeglang	Watermark on the wall of a house
20	F20	105.826547	-6.275825	4.85	-	-	Suka Ramai, Pandeglang	Broken roof tile of a villa's kitchen
21	F21	105.826853	-6.276961	1.25	-	-	Suka Ramai, Pandeglang	Watermark on the wall of a house
22	F22	105.827900	-6.273574	2.90	-	-	Sambolo, Pandeglang	Debris (fresh papaya leaf) on a tree
23	F23	105.827655	-6.274305	2.60	-	-	Sambolo, Pandeglang	Scratch of bark of a tree
24	F24	105.827525	-6.274409	3.60	-	-	Sambolo, Pandeglang	Broken twig of a tree
25	F25	105.836547	-6.199603	3.75	-	-	Bulakan, Serang	Scratch of bark of a tree
26	F26	105.833016	-6.210296	1.23	-	-	Bulakan, Serang	Watermark on the wall of a house
27	F27	105.841038	-6.298463	1.20	-	-	Carita Beach, Pandeglang	Broken banner for photo booth
28	F28	105.841058	-6.298815	2.50	-	-	Carita Beach, Pandeglang	Broken roof tile of a snorkeling rent shop
29	F29	105.830318	-6.316134	4.00	-	-	Mutiara Carita Hotel, Pandeglang	Broken coconut midrib near shoreline
30	F30	105.830325	-6.316660	3.10	-	-	Mutiara Carita Hotel, Pandeglang	Watermark on the wall of villa kitchen
31	F31	105.829851	-6.316504	4.85	-	-	Mutiara Carita Hotel, Pandeglang	Scratch of bark of a tree near shoreline
32	F32	105.829979	-6.316456	5.00	-	-	Mutiara Carita Hotel, Pandeglang	Broken coconut midrib near shoreline
33	F33	105.829215	-6.317133	3.50	-	-	Mutiara Carita Hotel, Pandeglang	Broken twig of a tree
34	F34	105.829175	-6.317366	3.34	-	-	Mutiara Carita Hotel, Pandeglang	Broken roof tile of a villa
35	F35	105.828639	-6.318095	3.75	-	-	Gading Nirwana Villa, Pandeglang	Debris (bag) on a tree at Gading Nirwana villa
36	F36	105.828445	-6.318715	5.50	-	-	Gading Nirwana Villa, Pandeglang	Broken roof tile of Gading Nirwana villa
37	F37	105.822073	-6.358663	2.75	-	-	Caringin Beach, Pandeglang	Broken twig of a tree
38	F38	105.822233	-6.358406	3.15	-	-	Caringin Beach, Pandeglang	Broken twig of a tree
39	F39	105.822545	-6.372932	1.10	-	-	Labuan Port, Pandeglang	Watermark on the wall of TPI PPP Labuan building
40	F40	105.826614	-6.416194	1.70	-	-	Cikaroeng Beach, Pandeglang	Watermark on the wall of a stall
41	F41	105.826269	-6.420829	1.08	-	-	Margagiri, Pandeglang	Watermark on the wall of Panorama Selat Sunda guest house
42	F42	105.811919	-6.464923	1.20	-	-	Cibungur, Pandeglang	Debris (fresh weeds and bag) on hence of a house

43	F43	105.687052	-6.522234	1.05	-	-	Tanjung Jaya, Pandeglang	In area of "pasar malam" (traditional fair): eyewitness account
44	F44	105.653580	-6.479668	4.80	-	-	Tanjung Lesung Resort, Pandeglang	Scratch of bark of a tree
45	F45	105.653905	-6.479859	4.95	-	-	Tanjung Lesung Resort, Pandeglang	Scratch of bark of a tree
46	F46	105.654720	-6.480059	2.30	-	-	Tanjung Lesung Resort, Pandeglang	Watermark on the wall of a multipurpose building of the resort
47	F47	105.640432	-6.503802	6.60	-	-	Cipenyu Beach, Pandeglang	Broken twig of *Pandanus odorifer*
48	F48	105.640419	-6.504018	5.00	-	-	Cipenyu Beach, Pandeglang	Broken twig of a tree
49	F49	105.640162	-6.504900	6.00	-	-	Cipenyu Beach, Pandeglang	Broken twig of a tree
50	F50	105.640464	-6.505401	1.00	-	-	Cipenyu Beach, Pandeglang	Broken twig of a tree
51	F51	105.640423	-6.505238	2.58	-	-	Cipenyu Beach, Pandeglang	Debris (fresh twig) on a tree
52	F52	105.641488	-6.504621	2.60	-	-	Cipenyu Beach, Pandeglang	Scratch of bark of a tree near hotel gate
53	F53	105.641456	-6.504185	2.56	-	-	Cipenyu Beach, Pandeglang	Scratch of bark of a tree
54	F54	105.640253	-6.503168	5.10	-	-	Cipenyu Beach, Pandeglang	Scratch of bark of a tree near Cipenyu boulder
55	F55	105.623226	-6.542170	3.30	-	-	Batu Hideung Beach, Pandeglang	Scratch of bark of a tree behind a hotel
56	F56	105.623379	-6.542129	3.53	-	-	Batu Hideung Beach, Pandeglang	Broken wall of a hotel
57	F57	105.618456	-6.617361	2.10	-	-	Banyuasih, Pandeglang	Scratch of bark of a tree
58	F58	105.617793	-6.619843	1.60	-	-	Banyuasih, Pandeglang	Debris (fresh weeds) on a coconut tree
59	F59	105.599488	-6.646446	5.85	-	-	Cisiih, Pandeglang	Broken waterboom building
60	F60	105.585145	-6.655973	4.75	-	-	Sumur, Pandeglang	Broken twig of a tree
61	F61	105.585353	-6.655795	5.25	-	-	Sumur, Pandeglang	Broken roof of a house
62	F62	105.586114	-6.655113	1.38	-	-	Sumur, Pandeglang	Broken window of a house
63	F63	105.586370	-6.655331	0.72	-	-	Sumur, Pandeglang	Watermark on the wall of a house
64	F64	105.586488	-6.655110	1.06	-	-	Sumur, Pandeglang	Watermark on the wall of a house
65	F65	105.585576	-6.654799	2.90	-	-	Sumur, Pandeglang	Broken roof of public toilet
66	F66	105.585552	-6.655041	3.15	-	-	Sumur, Pandeglang	Broken wall of a house
67	F67	105.572593	-6.679848	2.73	-	-	Kertajaya, Pandeglang	Watermark on the wall of Cinibung resort
68	F68	105.572542	-6.679808	2.25	-	-	Kertajaya, Pandeglang	Broken twig of a tree in front of resort
69	F69	105.587487	-5.751659	0.85	-	-	Maja, South Lampung	Watermark on the wall of a house
70	F70	105.587072	-5.752053	2.00	-	-	Maja, South Lampung	Dried leaves of a tree by seawater
71	F71	105.587038	-5.752164	2.00	-	-	Maja, South Lampung	Debris on coconut tree and sand in its midrib
72	F72	105.586607	-5.753841	1.80	-	-	Maja, South Lampung	Debris (cloting) on a tree
73	F73	105.587194	-5.753652	0.82	-	-	Maja, South Lampung	Watermark on the wall of a house
74	F74	105.587785	-5.752794	0.55	-	-	Maja, South Lampung	Watermark on the fence on a house
75	F75	105.587811	-5.751799	0.45	-	-	Maja, South Lampung	Watermark on the wall of Musholla Al-Furqan
76	F76	105.589913	-5.737631	2.20	-	-	Way Urang, South Lampung	Debris on a tree
77	F77	105.589916	-5.737494	2.20	-	-	Way Urang, South Lampung	Debris (fresh weeds) on a tree
78	F78	105.589952	-5.736212	3.90	-	-	Way Urang, South Lampung	Dried leaves of a tree by seawater
79	F79	105.589846	-5.736135	4.10	-	-	Way Urang, South Lampung	Scratch of bark of a tree
80	F80	105.589521	-5.734490	2.10	-	-	Way Urang, South Lampung	Debris (diaper) on a tree
81	F81	105.589238	-5.734038	2.60	-	-	Way Urang, South Lampung	Broken twig of Pandanus odorifer
82	F82	105.588990	-5.733584	2.30	-	-	Way Urang, South Lampung	Broken twig of Pandanus odorifer
83	F83	105.588878	-5.733349	2.15	-	-	Way Urang, South Lampung	Debris (packaging plastic) on a tree
84	F84	105.587500	-5.731201	2.05	-	-	Way Kiayi, South Lampung	Debris (fresh twig) on a tree
85	F85	105.587035	-5.730503	2.15	-	-	Way Kiayi, South Lampung	Debris (fresh weeds) on a remained building

86	F86	105.586493	-5.729601	2.88	-	-	Way Kiayi, South Lampung	Debris (fresh twig) on a Pandanus odorifer
87	F87	105.586416	-5.729409	2.24	-	-	Way Kiayi, South Lampung	Debris (packaging plastic) on a tree
88	F88	105.661842	-5.836995	3.82	-	-	Batu Balak, South Lampung	Broken wall of traditional fish hatchery
89	F89	105.661062	-5.836519	3.15	-	-	Batu Balak, South Lampung	Debris on the remained wall
90	F90	105.660542	-5.835730	2.54	-	-	Batu Balak, South Lampung	Scratch of bark of a tree
91	F91	105.659982	-5.835895	3.33	-	-	Kunjir, South Lampung	Broken twig of a tree at SDN 2 (elementary school)
92	F92	105.659578	-5.835282	1.44	-	-	Kunjir, South Lampung	Watermark on the wall of a house
93	F93	105.658080	-5.835432	2.25	-	-	Kunjir, South Lampung	Broken twig of a tree
94	F94	105.657472	-5.835092	4.46	-	-	Kunjir, South Lampung	Debris (sack) on a tree
95	F95	105.657179	-5.834773	2.54	-	-	Kunjir, South Lampung	Scratch of bark of a guava tree
96	F96	105.655319	-5.835032	3.05	-	-	Kunjir, South Lampung	Scratch of bark of a tree
97	F97	105.654070	-5.835363	2.10	-	-	Kunjir, South Lampung	Scratch of bark of a tree (above revetment)
98	F98	105.653339	-5.835333	2.68	-	-	Kunjir, South Lampung	Debris (cloting and curtain) on a tree
99	F99	105.651460	-5.836418	2.60	-	-	Kunjir, South Lampung	Debris (fresh weeds) on a tree
100	F100	105.651159	-5.836511	2.72	-	-	Kunjir, South Lampung	Broken both window and door of a house
101	F101	105.649145	-5.836813	2.05	-	-	Kunjir, South Lampung	Scratch of bark of a tree
102	F102	105.644980	-5.835529	2.25	-	-	Kunjir, South Lampung	Broken twig of a tree near a bridge
103	F103	105.643947	-5.835934	2.90	-	-	Kunjir, South Lampung	Broken twig of a tree
104	F104	105.640205	-5.836756	2.00	-	-	Kunjir, South Lampung	Broken twig and debris (packing plastic) on a tree
105	F105	105.637189	-5.838142	3.92	-	-	Way Muli, South Lampung	Broken twig of a guava tree
106	F106	105.636854	-5.838182	3.32	-	-	Way Muli, South Lampung	Debris (rope) on a tree
107	F107	105.636765	-5.838026	2.58	-	-	Way Muli, South Lampung	Scratch of bark of a tree
108	F108	105.636602	-5.838202	2.60	-	-	Way Muli, South Lampung	Debris (cloting) on a coconut tree
109	F109	105.634607	-5.838016	2.15	-	-	Way Muli, South Lampung	Debris (banana midrib) on a coconut tree
110	F110	105.632839	-5.837468	3.05	-	-	Way Muli, South Lampung	Debris on a tree
111	F111	105.105816	-5.770468	1.15	-	-	Sinar Maju, Tanggamus	Watermark on the guest house terrace (eyewitness account)
112	F112	105.106077	-5.770312	0.68	-	-	Sinar Maju, Tanggamus	Watermark on the wall of a house
113	F113	105.100232	-5.770776	0.50	-	-	Sinar Agung, Tanggamus	Watermark on a shack near shoreline
114	F114	105.099917	-5.771107	1.46	-	-	Sinar Agung, Tanggamus	Broken twig of a tree
115	F115	105.109351	-5.773583	1.05	-	-	Bandung Jaya, Tanggamus	Watermark on the wall of a house
116	F116	105.109148	-5.774083	1.84	-	-	Bandung Jaya, Tanggamus	Scratch of bark of a tree
117	F117	105.106666	-5.775991	1.30	-	-	Bandung Jaya, Tanggamus	Inundation depth on the road (eyewitness account)
118	R01	105.633862	-6.517582	-	-	14.90	Tanjung Jaya Beach, Pandeglang	Water line on the hill
119	R02	105.629937	-6.522420	-	-	9.39	Tanjung Jaya Beach, Pandeglang	Water line on the hill
120	R03	105.628406	-6.526900	-	-	11.14	Tanjung Jaya Beach, Pandeglang	Water line on the hill
121	H01	105.854724	-6.153412	-	5.16	-	Karang Suragak, Serang	Broken twig of a tree
122	H02	105.850006	-6.168573	-	3.20	-	Karang Bolong Beach, Serang	Watermark on the wall of a villa
123	H03	105.846338	-6.175847	-	3.74	-	Cipacung, Serang	Watermark on the wall of a house
124	H04	105.846756	-6.176050	-	3.22	-	Cipacung, Serang	Watermark on the wall of a house
125	H05	105.826499	-6.276083	-	6.63	-	Suka Ramai, Pandeglang	Broken twig of a tree
126	H06	105.826385	-6.276060	-	6.58	-	Suka Ramai, Pandeglang	Broken roof tile of a house
127	H07	105.826678	-6.288139	-	4.88	-	Suka Jadi, Pandeglang	Broken twig of a tree
128	H08	105.827176	-6.287947	-	2.92	-	Suka Jadi, Pandeglang	Watermark on the wall of a house

| 129 | H09 | 105.640194 | -6.504876 | - | 9.56 | - | Cipenyu Beach, Pandeglang | Broken twig of a tree |
| 130 | H10 | 105.640383 | -6.505218 | - | 8.54 | - | Cipenyu Beach, Pandeglang | Broken twig of a tree |

Appendix B. Building Damages

No	Building Code	Location	Coordinate Long	Coordinate Lat	Building Function	Building Type	Flow Depth (m)	DC
1	B1	Bulakan Pondok Beach,	105.846387	-6.175758	Villa	Confined Masonry	2.08	3
2	B2	Bulakan Pondok Beach,	105.846551	-6.176082	House	Timber house	2.08	4
3	B3	Bulakan Pondok Beach,	105.846470	-6.176195	House	Timber house	2.08	4
4	B4	Bulakan, Serang	105.832935	-6.210453	House	Timber house	1.23	3
5	B5	Bulakan, Serang	105.833016	-6.210296	House	Timber house	1.23	2
6	B6	Suka Ramai, Pandeglang	105.827204	-6.276455	Villa's kitchen	Confined Masonry	4.85	3
7	B7	Karang Bolong Beach, Sera	105.849609	-6.168915	Villa	Confined Masonry	1.48	2
8	B8	Suka Ramai, Pandeglang	105.826926	-6.276281	House	Confined Masonry	1.95	2
9	B9	Suka Ramai, Pandeglang	105.827170	-6.276110	House	Confined Masonry	1.95	2
10	B10	Suka Ramai, Pandeglang	105.826398	-6.276132	House	Confined Masonry	4.80	3
11	B11	Suka Ramai, Pandeglang	105.826577	-6.276212	House	Confined Masonry	4.80	3
12	B12	Labuan Port, Pandeglang	105.822271	-6.372431	House	Timber house	1.10	3
13	B13	Labuan Port, Pandeglang	105.822312	-6.372458	House	Confined Masonry	1.10	2
14	B14	Gading Nirwana Villa,	105.828445	-6.318715	Villa	Confined Masonry	5.50	3
15	B15	Gading Nirwana Villa,	105.828944	-6.318459	Villa	Confined Masonry	5.50	3
16	B16	Gading Nirwana Villa,	105.829049	-6.317649	Villa	Confined Masonry	5.50	4
17	B17	Gading Nirwana Villa,	105.828974	-6.317821	Villa	Confined Masonry	5.50	4
18	B18	Gading Nirwana Villa,	105.828825	-6.317949	Villa	Confined Masonry	5.50	4
19	B19	Gading Nirwana Villa,	105.828439	-6.318949	Villa	Confined Masonry	5.50	4
20	B20	Gading Nirwana Villa,	105.828431	-6.31917	Villa	Confined Masonry	5.50	4
21	B21	Gading Nirwana Villa,	105.828443	-6.319373	Villa	Confined Masonry	5.50	4
22	B22	Gading Nirwana Villa,	105.828479	-6.319607	Villa	Confined Masonry	5.50	4
23	B23	Gading Nirwana Villa,	105.828452	-6.319836	Villa	Confined Masonry	5.50	4
24	B24	Mutiara Carita Hotel,	105.830175	-6.31652	Villa	Confined Masonry	4.85	3
25	B25	Mutiara Carita Hotel,	105.830421	-6.316628	Villa Restourant	Timber house	3.34	3
26	B26	Mutiara Carita Hotel,	105.829243	-6.31744	Villa	Confined Masonry	3.34	3
27	B27	Mutiara Carita Hotel,	105.830265	-6.31697	Villa	Confined Masonry	3.34	3
28	B28	Mutiara Carita Hotel,	105.830639	-6.316496	Villa	Confined Masonry	3.34	3
29	B29	Mutiara Carita Hotel,	105.830001	-6.316645	Villa	Timber house	4.85	4
30	B30	Mutiara Carita Hotel,	105.829877	-6.316725	Villa	Timber house	4.85	4
31	B31	Mutiara Carita Hotel,	105.829715	-6.316897	Villa	Timber house	4.85	4
32	B32	Mutiara Carita Hotel,	105.829551	-6.317075	Villa	Timber house	4.85	4
33	B33	Mutiara Carita Hotel,	105.829387	-6.317237	Villa	Timber house	4.85	4
34	B34	Mutiara Carita Hotel,	105.829902	-6.317026	Villa	Timber house	4.85	4
35	B35	Mutiara Carita Hotel,	105.829705	-6.317263	Villa	Timber house	4.85	4
36	B36	Mutiara Carita Hotel,	105.829724	-6.317553	Villa	Timber house	4.85	4
37	B37	Mutiara Carita Hotel,	105.830081	-6.316815	Villa	Confined Masonry	4.85	3
38	B38	Cipenyu Beach,	105.64079	-6.503614	Hotel	Confined Masonry	6.60	3
39	B39	Cipenyu Beach,	105.641812	-6.504184	House	Timber house	2.56	4
40	B40	Batu Hideung Beach,	105.623447	-6.542079	Hotel	Confined Masonry	3.53	3
41	B41	Datu Carita Beach,	105.829152	-6.262584	Warehouse	Frame steel	2.30	3
42	B42	Cisiih, Pandeglang	105.599653	-6.647483	Security Post	Confined Masonry	1.70	3
43	B43	Cisiih, Pandeglang	105.599488	-6.646446	Waterboom	Confined Masonry	5.86	3
44	B44	Sumur, Pandeglang	105.587639	-6.654235	House	Confined Masonry	3.15	3
45	B45	Sumur, Pandeglang	105.585353	-6.655795	House	Confined Masonry	5.25	3
46	B46	Sumur, Pandeglang	105.585512	-6.655944	House	Timber house	1.38	2
47	B47	Sumur, Pandeglang	105.586114	-6.655113	House	Timber house	1.38	3
48	B48	Sumur, Pandeglang	105.585576	-6.654799	Public Toilet	Confined Masonry	2.90	4
49	B49	Sumur, Pandeglang	105.585111	-6.655604	House	Timber house	4.75	4
50	B50	Sumur, Pandeglang	105.585052	-6.655685	House	Timber house	4.75	
51	B51	Sumur, Pandeglang	105.584993	-6.655721	House	Timber house	4.75	4
52	B52	Sumur, Pandeglang	105.584939	-6.655751	House	Timber house	4.75	4
53	B53	Sumur, Pandeglang	105.584868	-6.655818	House	Timber house	4.75	4
54	B54	Sumur, Pandeglang	105.587293	-6.653920	House	Timber house	4.75	4
55	B55	Sumur, Pandeglang	105.587187	-6.654020	House	Timber house	4.75	4
56	B56	Sumur, Pandeglang	105.587124	-6.654063	House	Timber house	4.75	4
57	B57	Kertajaya, Pandeglang	105.585552	-6.655041	Hotel	Confined Masonry	3.15	3
58	B58	Maja, Kalianda-Lampung	105.58715	-5.751505	House	Confined Masonry	2.00	3
59	B59	Maja, Kalianda-Lampung	105.587331	-5.751383	warehouse	Confined Masonry	2.00	3
60	B60	Maja, Kalianda-Lampung	105.587487	-5.751659	House	Confined Masonry	0.85	0
61	B61	Maja, Kalianda-Lampung	105.587162	-5.752162	House	Confined Masonry	2.00	3
62	B62	Maja, Kalianda-Lampung	105.587108	-5.752279	House	Confined Masonry	2.00	3
63	B63	Maja, Kalianda-Lampung	105.587811	-5.751799	Mosque	Confined Masonry	0.45	0
64	B64	Maja, Kalianda-Lampung	105.587194	-5.753652	House	Confined Masonry	0.82	0
65	B65	Way Urang, Kalianda-	105.589884	-5.736296	House	Confined brick	2.20	3
66	B66	Kunjir, Rajabasa-Lampung	105.660001	-5.835786	School	Confined Masonry	3.33	3
67	B67	Kunjir, Rajabasa-Lampung	105.659578	-5.835282	House	Confined Masonry	1.44	3
68	B68	Kunjir, Rajabasa-Lampung	105.658894	-5.835389	House	Confined Masonry	2.54	2
69	B69	Kunjir, Rajabasa-Lampung	105.656977	-5.834338	House	Confined Masonry	2.54	2
70	B70	Kunjir, Rajabasa-Lampung	105.655330	-5.834946	House	Timber house	2.54	3
71	B71	Kunjir, Rajabasa-Lampung	105.655310	-5.834685	House	Confined Masonry	2.54	2
72	B72	Way Muli, Rajabasa-	105.652452	-5.835945	Mosque	Confined Masonry	2.60	3
73	B73	Way Muli, Rajabasa-	105.652641	-5.835994	House	Confined Masonry	2.60	3
74	B74	Way Muli, Rajabasa-	105.651743	-5.836167	House	Confined Masonry	2.60	3
75	B75	Way Muli, Rajabasa-	105.650652	-5.836636	House	Confined Masonry	2.72	2
76	B76	Way Muli, Rajabasa-	105.650306	-5.836948	House	Confined Masonry	2.72	3
77	B77	Way Muli, Rajabasa-	105.650658	-5.836925	House	Confined brick	2.25	3
78	B78	Way Muli, Rajabasa-	105.650647	-5.836617	House	Confined Masonry	1.25	0
79	B79	Way Muli, Rajabasa-	105.650748	-5.836632	House	Confined Masonry	1.25	0
80	B80	Way Muli, Rajabasa-	105.649514	-5.836832	House	Confined Masonry	2.72	2
81	B81	Way Muli, Rajabasa-	105.649297	-5.836305	House	Confined Masonry	2.05	1
82	B82	Way Muli, Rajabasa-	105.645829	-5.835347	House	Confined Masonry	3.25	3
83	B83	Way Muli, Rajabasa-	105.645897	-5.835398	House	Confined Masonry	3.25	3
84	B84	Way Muli, Rajabasa-	105.64417	-5.835387	House	Confined Masonry	2.25	3
85	B85	Way Muli, Rajabasa-	105.641748	-5.835945	House	Confined Masonry	2.90	3
86	B86	Way Muli, Rajabasa-	105.637209	-5.838089	Mosque	Confined Masonry	3.92	4
87	B87	Way Muli, Rajabasa-	105.63704	-5.837943	House	Confined Masonry	3.92	3
88	B88	Way Muli, Rajabasa-	105.634178	-5.837983	House	Confined Masonry	2.15	2
89	B89	Way Muli, Rajabasa-	105.634003	-5.837899	House	Confined Masonry	2.15	3
90	B90	Bandung Jaya,	105.109351	-5.773583	House	Timber house	1.85	3
91	B91	Maja, Kalianda-Lampung	105.588860	-5.745037	House	Confined Masonry	0.20	0
92	B92	Maja, Kalianda-Lampung	105.587354	-5.749341	House	Confined Masonry	0.25	0
93	B93	Maja, Kalianda-Lampung	105.587902	-5.751532	House	Confined Masonry	0.30	0
94	B94	Kunjir, Rajabasa-Lampung	105.654917	-5.834229	House	Confined Masonry	0.30	0
95	B95	Kunjir, Rajabasa-Lampung	105.657019	-5.834202	House	Confined Masonry	0.40	0
96	B96	Kunjir, Rajabasa-Lampung	105.662337	-5.836057	House	Confined Masonry	0.50	0
97	B97	Kunjir, Rajabasa-Lampung	105.663067	-5.836901	House	Confined Masonry	0.50	0
98	B98	Way Muli, Rajabasa-	105.638753	-5.836537	House	Confined Masonry	0.60	0

Appendix C. Tsunami Boulders

No	Boulder Code	Location	Coordinate (source) lon	Coordinate (source) lat	Coordinate (drifted) lon	Coordinate (drifted) lat	Boulder Material	Size (m) Diameter	Size (m) Long	Size (m) Width	Size (m) High	Volume (m³)	Distance (m)	Density (kg/m³)	Weight (kg)	A	Est. Velocity (m/s)
1	Bo-1	Karang Suraga, Serang	105.854606	-6.152928	105.85487	-6.15298	Rubble mound	0.64	-	-	0.43	0.137	28	2650	363.550	0.322	2.78
2	Bo-2	Karang Bolong Beach,	105.84953	-6.16854	105.84958	-6.16863	Concrete	-	1.42	0.35	0.37	0.184	12	2200	404.558	0.5254	2.30
3	Bo-3	Bulakan, Serang	105.83254	-6.21030	105.83278	-6.21042	Rubble mound	1.12	-	-	0.55	0.735	32	2650	1948.401	0.986	3.68
4	Bo-4	Cipenyu Beach, Tanjung	105.639867	-6.503775	105.64152	-6.50400	Coral reef	0.42	-	-	0.28	0.039	185	1450	56.220	0.139	1.67
5	Bo-5	Cipenyu Beach, Tanjung	105.639725	-6.502764	105.60046	-6.50304	Coral reef	2.88	-	-	2.62	12.501	87	1450	18126.914	6.517	4.37
6	Bo-6	Maja, Kalianda-South	105.58701	-5.75224	105.58719	-5.75230	Coral reef	0.2	-	-	0.15	0.004	20	1450	6.071	0.031	1.15
7	Bo-7	Maja, Kalianda-South	105.58683	-5.75264	105.58703	-5.75276	Concrete	-	0.75	0.55	0.40	0.165	26	2200	363	0.3	2.88
8	Bo-8	Kunjir, Rajabasa-South	105.65863	-5.83572	105.65868	-5.83556	Rubble mound	1.12	-	-	0.57	0.735	18	2650	1948.401	0.986	3.68